The *In Vivo* Source of Type I and Type III IFNs is Pathogen Dependent

Marvin J. Sandoval[1,4], Hsiang-Chi Tseng[2], Heidi P. Risman[2], Sergey Smirnov[3] Qing Li[3], Jian-Da Lin[3,5], Amariliz Rivera[6], Russell K. Durbin[2], Sergei V. Kotenko[3] and Joan E. Durbin[2*,]

[1.] Immunology and Inflammation Graduate Program, New York University School of Medicine, 550 1st Ave., New York, NY, USA.

[2.] Department of Pathology, Immunology and Laboratory Medicine, Rutgers – New Jersey Medical School, 185 South Orange Ave., Newark, NJ, USA

[3.] Department of Microbiology, Biochemistry and Molecular Genetics, Rutgers – New Jersey Medical School, 205 S. Orange Ave., Newark, NJ, USA

[4.] Current Address: Autoimmunity and Inflammation Program, Hospital for Special Surgery, New York, NY 10021

[5.]Current Address: Department of Biochemical Science and Technology, College of Life Science, National Taiwan University, Taipei City, Taiwan.

[6.] Department of Pediatrics, Rutgers – New Jersey Medical School, 205 S. Orange Ave., Newark, NJ, USA

* Corresponding author

durbinje@njms.rutgers.edu (JED)

Abstract

Type I (-α, β) and type III (-λ) interferons (IFNs) are produced in response to virus infection and upregulate a largely overlapping set of IFN stimulated genes which mediate the protective effects of these antiviral cytokines. *In vitro* studies have demonstrated the redundancy of these two cytokine families which activate the same transcription factor, IFN stimulated gene factor 3 (ISGF3), via distinct ligands and receptors. However, *in vivo*, these IFN types do have distinct functions based on receptor distribution, but also ligand availability. Using a newly generated IFN-λ reporter mouse strain we have observed that both type I and type III IFNs are produced in response to respiratory tract infection by Newcastle disease virus (NDV) and influenza A virus (IAV). In the case of NDV these IFNs are synthesized by different cell types. Type I IFNs are produced primarily by alveolar macrophages, type III IFNs are made only by epithelial cells, and production of either is dependent on MAVS. While epithelial cells of the respiratory tract represent the primary target of IAV infection, we found that they did not significantly contribute to IFN-λ production, and IFN-λ protein levels were largely unaffected in the absence of MAVS. Instead we found that pDCs, a cell type known for robust IFN-α production via TLR/MyD88 signaling, were the major producers of IFN-λ during IAV infection, with pDC depletion during influenza infection resulting in significantly reduced levels of both IFN-α and IFN-λ. In addition, we were able to demonstrate that pDCs rely on type I IFN for optimal IFN-λ production. These studies therefore demonstrate that the *in vivo* producers of Type III IFNs in response to respiratory virus infection are pathogen dependent, a finding which may explain the varying levels of cytokine production induced by different viral pathogens.

Introduction

The antiviral activity of the type I interferons (IFN-α/β) has been appreciated since their discovery in 1957 [1, 2]. The more recent discovery of type III IFNs (IFN-λ) [3] [4], a new IFN family with its own distinct receptor but mediating the same antiviral response, has led to a reevaluation of our understanding of innate immune responses. The IFN-λ receptor, comprised of the IFN-lambda receptor (IFNLR) chain and the IL-10R2 chain, is expressed on most epithelial cells, but not ubiquitously found on all cell types like the IFN-alpha receptors (IFNAR) 1 and 2. The type III IFNs act to protect mucosal surfaces, the point of entry for many viral pathogens, but their source(s), and the stimuli leading to their production are not yet well characterized [7, 8]. To better understand the relative contributions of type I and type III IFNs to antiviral protection, we generated an IFN-λ reporter mouse, *Ifnl2*$^{gfp/gfp}$, and used this strain to examine the relative contribution of various cell types to the production of these cytokines. This approach was inspired by the work of Kumagai *et al*. [5] who demonstrated that alveolar macrophages produce the bulk of IFN-α following pulmonary infection with Newcastle disease virus (NDV) using mice expressing GFP under the control of the *Ifna6* promoter. Similar results were obtained following infection of these *Ifna6*$^{gfp/+}$ mice with respiratory syncytial virus (RSV) [6].

Multiple studies have demonstrated that type I and type III IFNs are induced *in vitro* by the same stimuli, e.g. virus infection and TLR ligand exposure [7] [8], but it is not yet known if induction consistently follows the same pathways following virus infection *in vivo*. Making use of *Ifnl2*$^{gfp/gfp}$ mice we have confirmed Kumagai's observation that

alveolar macrophages are the major source of IFN-α during NDV infection, but also observed that this cell type produces no IFN-λ. IFN-λ in this infection is entirely derived from respiratory epithelial cells in a MAVS-dependent manner. The finding that IFN-λ is preferentially produced by polarized epithelial cells *in vitro* [9] has also been observed in mouse models [10]. These published results support the notion that, despite their activation of the same antiviral pathway, IFN-α/β and IFN-λ are produced by different cell types in response to the same stimulus.

In this study we used the *Ifnl2*$^{gfp/gfp}$ reporter mice to test the generality of this hypothesis with a number of viruses. In both the NDV and rhesus rotavirus (RRV) infections we observed IFN-λ production by the IFN-λ responsive cells lining the target tissue, emphasizing the important role for this cytokine in protection of the epithelial barrier. This pattern of IFN expression was not recapitulated in the murine model of influenza A virus (IAV) infection, where a significant proportion of IFN-λ induced by infection was produced by pDCs in a MAVS-independent manner. Taken together our studies show that the source of type I and type III IFNs *in vivo* is pathogen dependent, and not defined by the route of infection or the tropism of the infecting virus.

Results

Generation and Characterization of the IFN-λ reporter mouse

To identify IFN-λ-producing cell populations *in vivo*, we generated an IFN-λ reporter mouse by replacing the coding region of *ifnl2* with an *eGFP-Neo* cassette through homologous recombination, while maintaining the *ifnl2* promoter and UTR regions intact (Fig 1A). The FRT sites flanking the neo gene allowed its removal by crossing mice carrying the targeted allele with mice expressing the FLP-recombinase to generate animals lacking the Neo gene while simultaneously carrying the GFP-targeted allele. Mice heterozygous for the eGFP-targeted allele were crossed to generate mice homozygous for the targeted allele. Homozygous *ifnl2*$^{eGFP/eGFP}$ knockin mice can no longer produce IFN-λ2, but still retain functional *ifnl3* gene loci. Genotypes were determined by conventional PCR using primers targeting the IFN-λ locus and the eGFP transgene (Fig 1A, B).

Human pDCs secrete high levels of both type I and type III IFNs when stimulated by TLR ligands or virus infection [11], so characterization of the reporter strain was initiated by Newcastle disease virus (NDV) infection of Flt3-ligand (FLT3L) cultured bone marrow derived dendritic cells. NDV is an avian paramyxovirus known to induce high levels of type I IFNs in many cell types including murine pDCs [5, 12], so we used this system to ask whether GFP expression correlated with IFN-λ production upon induction by virus infection.

GFP expression following virus inoculation was detected by fluorescence microscopy (Fig 1C), as well as flow cytometry (Fig 1D). A Fluorescence Activated Cell Sorter (FACS) was used to separate NDV-treated, FLT3L-cultured DCs into GFP- and GFP+ populations

for RNA extraction and subsequent qRT-PCR analysis of IFN-λ3 and eGFP transcripts (Fig 1D). This analysis confirmed that IFN-λ3 and eGFP transcripts were enriched only in GFP+ cells, demonstrating that GFP fluorescence from reporter cells reflected IFN-λ production.

We also explored GFP induction following virus infection of epithelial cells. Primary kidney epithelial cells derived from *ifnl2*$^{gfp/gfp}$ reporter mice were cultured *in vitro* and infected with NDV, respiratory syncytial virus (RSV), rhesus rotavirus (RRV) or influenza A virus (Fig 1E). At 24 hours post-infection, all infected cultures contained GFP+ cells, but for all viruses the percentage of GFP+ cells was relatively small, even at higher MOIs. A similar effect was observed in FLT3L cultured DCs (data not shown), suggesting that during a virus infection, not all cells capable of producing IFN-λ go on to do so as has been found for IFN-α [13].

A small population of CD8α DCs produce IFN-λ in response to poly I:C treatment *in vivo*

Production of IFN-λ by different cell types has been detected in response to a wide variety of stimuli or pathogens *in vitro* [14-16]. Taken together, these publications demonstrate that many cell types have the capacity to produce type III IFNs under the appropriate conditions. However, reports investigating the cellular sources of IFN-λ in a whole animal in response to TLR ligands or virus infections are few. One such study identified splenic CD8α+ dendritic cells as the main producers of IFN-λ in mice that were treated intravenously (i.v.) with the TLR3 agonist, poly I:C [17]. We carried out a similar experiment using our IFN-λ reporter mouse model to determine whether we could confirm

that result by following GFP expression. Cohorts of *Ifnl2*$^{gfp/gfp}$ reporter mice were injected i.v. with 100 µg of poly I:C or PBS, and their splenocytes harvested six hours later. Using antibodies to the cell surface markers CD11b, CD11c, CD8α, B220, and Siglec H, we identified pDC, CD8α DC, and cDC subsets, and found, as expected, that GFP expression was mainly confined to the CD8α DC populations (Fig 2). Interestingly, IFN-λ-producing (GFP+) CD8α DCs made up only 6% of the entire CD8α DC population; GFP expression by pDCs and cDCs was minimal. This result is consistent with the observation of Lauterbach *et al*. [17] that CD8α DCs are by the far the most significant contributor to IFN-λ production in response to poly I:C, supporting the use of the *Ifnl2*$^{gfp/gfp}$ mouse strain to determine the source of IFN-λ *in vivo*. No upregulation of GFP was found in animals receiving PBS.

Intestinal epithelial cells produce IFN-λ in response to rotavirus infection *in vivo*

As both type I and type III IFNs are produced in response to many different virus infections *in vivo* [14] [7], we wished to investigate the cellular sources of type III IFNs during virus infection of mucosal surfaces such as the gastrointestinal tract and the respiratory tract. Rotavirus is a double-stranded RNA virus that primarily infects intestinal epithelial cells and is one of the leading causes of severe diarrhea in young children in the developing world [18]. Several studies have shown the importance of IFN-λ responses, along with type I IFNs, in controlling rotavirus replication [19, 20]. Here, we explored the *in vivo* source of IFN-λ during rhesus rotavirus (RRV) infection of suckling mice. The kinetics of IFN induction by RRV was first determined using Mx2-Luciferase mice, a reporter mouse strain that allows visualization and quantification of IFN responses by

measuring luciferase activity driven by the promoter of the interferon-stimulated gene Mx2 [21]. By this approach, a robust interferon response was detected as early as 12 hours post-infection, peaking at 24 hours, and subsiding after 48 hours (Fig 3A&B). Consistent with this observation, IFN-λ protein was detected in the small intestine of rotavirus-infected WT 129SvEv mice 24 hours post-infection by ELISA (Fig 3C). To determine the source of IFN-λ induced by RRV, intestines were harvested from infected IFN-λ reporter mice 24 hours post-inoculation and analyzed by immunohistochemistry. Formalin-fixed, paraffin-embedded tissue sections from mock-infected or RRV-infected IFN-λ reporter mice were stained with antibodies against GFP and RRV antigens (Fig 3E). GFP+ cells were present only in tissues harvested from RRV-infected IFN-λ reporter mice, and absent from the intestines of mock-infected IFN-λ reporter mice, or RRV-infected WT 129SvEv animals. GFP expression in RRV-infected IFN-λ reporter mice was found exclusively in the intestinal epithelial cells. RRV-infected epithelial cells were found in both RRV-infected IFN-λ reporter mice and RRV-infected WT controls, confirming successful infection of these animals. These results support the hypothesis that epithelial cells are the primary source of IFN-λ during RRV infection. As IFN-λ reporter mice lack the *ifnl2* locus but have an intact *ifnl3* locus, we compared RRV titers from the small intestine of IFN-λ reporter and WT 129SvEv animals, and found no difference in the amount of virus detected (Fig 3D). Thus the reporter mice are phenotypically normal, without enhanced susceptibility to virus infection or elevated virus loads.

178 **Airway epithelial cells produce IFN-λ in response to NDV infection *in vivo***

179 Next, we sought to investigate IFN-λ production during virus infection of the respiratory
180 tract, another mucosal compartment that serves as a major portal for virus entry. Our lab
181 and others have reported that both type I and type III IFNs are produced in response to
182 respiratory virus infections [22, 23]. In the lung, as in the intestine, both IFN types appear
183 to be important for antiviral protection of the respiratory tract, as mice deficient in both
184 type I and type III IFN receptors demonstrate significantly elevated viral burdens upon
185 virus challenge [24, 25]. To determine whether the airway lining cells are major IFN-λ
186 producers during respiratory virus infection *in vivo*, we inoculated IFN-λ reporter mice with
187 Newcastle disease virus (NDV), a virus known to induce high levels of type I IFNs in
188 mammals [26, 27]. At 24 hours post-infection, lungs from mock-infected or NDV-infected
189 mice were harvested and processed to generate single cell suspensions. IFN-λ-producing,
190 epithelial cell adhesion molecule (EpCAM)+ epithelial cells were assayed for GFP
191 expression by flow cytometry. Only epithelial cells from NDV-infected reporter mice were
192 GFP+ (Fig 4A), with approximately 15% of lung epithelial cells in the IFN-λ reporter mice
193 expressing IFN-λ in response to infection *in vivo* (Fig. 4B). ELISA measurements of IFN-
194 λ protein present in bronchoalveolar lavage samples (BALs) from these same animals
195 also demonstrated robust IFN-λ secretion in response to NDV infection, with > 10 ng/ml
196 of IFN-λ protein detected (Fig 4C).

197 As with our rotavirus studies, we looked for GFP+ cells in tissue sections prepared from
198 IFN-λ reporter mice that were mock or NDV-infected. As before, lung tissue sections were
199 stained using antibodies against GFP and viral antigens (Fig 4D). This histological
200 analysis confirmed our flow cytometry results, showing that GFP expression was limited

to the columnar epithelial cells that line the bronchi and bronchioles of the lung. The same cell type expressed both NDV and GFP protein in infected lungs. Interestingly, while rare cells stained with antibodies to both GFP and NDV proteins, most cells in the infected airway showed either GFP or NDV staining. To be certain that elimination of IFN-λ2 in our reporter mouse was not skewing our results, we compared total IFN-α and IFN-λ production in BAL samples from NDV-infected WT and reporter mice and saw no significant difference between the strains (Fig 5).

Immune cells are not a significant source of IFN-λ during NDV infection *in vivo*

IFN-λ synthesis by dendritic cells and monocytes exposed to viruses and pattern recognition receptor (PRR) agonists *in vitro* has been reported [7, 8, 11, 28]. So while results from our flow cytometry and histology studies using the IFN-λ reporter mice clearly demonstrated GFP expression from bronchial epithelial cells during NDV infection *in vivo*, we wished to determine whether there was also a contribution from innate immune cells in this model. To do this we used a panel of antibodies targeting cell surface markers to assess IFN-λ production, or GFP expression, by neutrophils ($CD45^+$ $F4/80^-$ $Ly6G^+$), eosinophils ($CD45^+$ $F4/80^+$ $SiglecF^+$ CD11c-), monocyte-derived macrophages ($CD45^+$ $F4/80^+$ $SiglecF^-$ $CD11c^+$) and alveolar macrophages ($CD45^+$ $F4/80^+$ Siglec F^+ $CD11c^+$) purified from the lungs of NDV-infected IFN-λ reporter mice 24 hours post-infection. GFP expression was minimal in all of these cell types (Fig 6), and therefore it is unlikely that they are contributing significantly to IFN-λ production in this setting.

We were particularly intrigued by the lack of GFP expression in alveolar macrophages from NDV-infected IFN-λ reporter mice. Previously published reports using an IFN-α

reporter mouse have identified alveolar macrophages as the major IFN-α-producing cell population during NDV and RSV infections *in vivo* [5, 6]. The results of our experiment demonstrate that alveolar macrophages do not contribute to IFN-λ production stimulated by NDV infection *in vivo*, suggesting that alveolar macrophages preferentially upregulate type I IFNs. To confirm this observation we carried out NDV infections in WT 129 SvEv mice and looked for induced IFN-λ expression in both epithelial cells and alveolar macrophages. Lungs from mock- or NDV-infected mice were harvested 24 hrs post-infection, and epithelial cells (CD45- EpCAM+) and alveolar macrophages (CD45+ F4/80+ SiglecF+ CD11c+) were sort purified by FACS. RNA from the sorted cell populations was used to synthesize cDNA for qPCR analysis which showed that IFN-λ transcripts were present only in the epithelial cell fraction isolated from NDV-infected mice (Fig 7). IFN-λ transcripts were not detected in the alveolar macrophage fraction from either mock-infected or NDV-infected mice, further confirming the readout from the IFN-λ reporter mouse strain. As an alternative approach to assessing IFN-λ production induced by virus, we used *in situ* hybridization to detect IFN-λ mRNA in lung sections from infected animals (Fig 8). IFN-λ RNA was found in bronchial epithelial cells of NDV-infected mice and not mock-infected animals. Taken together, the results from our qRT-PCR and *in situ* hybridization studies lead to the conclusion that only epithelial cells, and not alveolar macrophages, are responsible for IFN-λ production during NDV infection.

To ensure that our study produced results consistent with the work of Kumagai *et al*. [5], we also assayed RNA purified from the sorted epithelial cell and alveolar macrophage populations (Fig 8A) for the presence of IFN-α transcripts. As expected, induction of IFN-α mRNAs were observed only in alveolar macrophages (Fig 8C&D).

247

248 **IFN production by alveolar macrophages *ex vivo***

249 Noting the inability of the alveolar macrophage population to synthesize type III IFNs
250 in the course of NDV infection, we wished to determine whether these cells were
251 intrinsically unable to produce IFN-λ in response to NDV, or whether extrinsic factors in
252 the lung microenvironment were restricting their production of IFN-λ. To ask this question,
253 alveolar macrophages were purified from the lungs of naïve 129 SvEv mice by
254 collagenase digestion and FACS sorting (Fig 9A) then mock-infected, or infected with
255 NDV at an MO1=10, for 24 hours. The cells were then collected for RNA extraction and
256 assayed by qPCR for the presence of IFN-λ transcripts. RNA isolated from a rodent cell
257 line constitutively expressing FLAG-tagged mIFN-λ2, was used as a positive control. This
258 analysis failed to detect IFN-λ expression from either mock-infected or NDV-infected
259 alveolar macrophages (Fig 9B), a result confirmed by ELISA assay of media from the
260 infected alveolar macrophage cultures (Fig 9C). Assay of the same samples showed high
261 levels of IFN-α in media harvested from NDV-infected alveolar macrophages (Fig 9C).
262 These results demonstrate that the same stimulus results in the production of either type
263 I or type III IFN in a cell-type specific manner.

264

265 **Plasmacytoid dendritic cells, and not epithelial cells, are the major producers of**
266 **IFN-λ during influenza A virus (IAV) infections *in vivo***

267 Intranasal administration of the non-replicating NDV allowed us to examine type I and
268 type III IFN production following initial exposure, without regard to virus spread. However
269 we also wished to use the *Ifnl2*$^{gfp/gfp}$ reporter mouse strain to characterize IFN-λ induction

by influenza A virus (IAV), a virus capable of robust replication and spread in this species. Published studies have reported co-production of type I and type III IFNs from both pDCs [11] and epithelial cells [23, 29] exposed to IAV *ex vivo,* and we wished to characterize the *in vivo* source(s) of these cytokines. Lung homogenates from *Ifnl2*$^{gfp/gfp}$ mice infected with the WSN strain of IAV (10^6 pfu) were prepared 48 hours post infection, and assayed by flow cytometry for GFP expression. By this method, measurable GFP expression was detected only in the pDC subset (CD45+/CD11c+/CD11b-/B220+/PDCA1+) and not in epithelial cells (Fig 10A-C).

Given the data obtained with NDV, and a recent study which concluded that epithelial cells are the primary source of IFN-λ in IAV infection [30], we considered the possibility that the more numerous epithelial cells might produce lower levels of IFN-λ on a per cell basis, below the level of detection by GFP expression, but still contribute to overall production of this cytokine. We approached this question in two ways. Using the sorting strategy shown in Figure 10 B & C, epithelial cells and pDCs from lungs of IAV-infected WT mice and controls were obtained, and RNA harvested from these populations was assayed by qRT-PCR for the presence of *Ifnl2/3* transcripts. As shown in Figure 10D, while IFN-λ2/3 mRNA could be detected in EpCAM+ cells from infected animals, pDCs appeared to be the predominant source of both IFN-α and IFN-λ. This result was consistent with ISH hybridization studies using formalin-fixed lung tissues form IAV-infected WT and reporter mice. Immunofluorescence studies showed diffuse positive staining for influenza antigen in airway lining epithelium, and oligonucleotide probes did detect rare IFN-λ2/3 expressing epithelial cells (Fig 10E) in animals infected with the WSN strain of IAV. A similar GFP expression pattern in pDCs and epithelial cells was observed

293 by flow cytometry in animals infected with the PR8 strain, in the presence or absence of
294 the NS1 gene (Fig 11) 48 hrs post-infection, but we were not able to detect *ifnl* transcripts
295 by ISH in PR8-infected epithelial cells (data not shown).
296 To determine the relative contribution of these sources, we generated marrow chimeras
297 using bone marrow harvested from newly generated IFN-λ ligand deficient mice, *ifnl-/-* ,
298 lacking both the *ifnl2* and *ifnl3* alleles (See Supplemental Fig. 2). Lethally irradiated WT
299 mice were reconstituted with bone marrow harvested from either WT or *ifnl-/-* animals.
300 Chimeric mice were then challenged with IAV, 10^5 pfu of WSN, and BALs collected 48
301 hours post infection were assayed for the presence of IFN-λ by ELISA. IAV-infected mice
302 reconstituted with *ifnl-/-* bone marrow showed significantly reduced levels of IFN-λ protein
303 compared with IAV-infected animals which received WT bone marrow (Fig 12)
304 demonstrating that ~ 30%, of IFN-λ produced in response to IAV is derived from the
305 epithelial compartment. To further pinpoint the source of this cytokine, WT mice were
306 depleted of pDCs prior to IAV infection with anti-PDCA1 antibody, or a Rat IgG Isotype
307 control (Fig 13A). Post infection measurements of BAL IFN-λ show a significant decrease
308 in IFN-λ production in the absence of pDCs at 24 hrs post-infection, ~ 60% (Fig 13B),
309 consistent with the data obtained by generation of bone marrow chimeras.
310
311
312 **Pathway activation by virus**
313 As IFN-λ induction by NDV occurred only in CD45- EpCAM+ cells, and IFN-α induction
314 only in alveolar macrophages in NDV infection, we hypothesized that production of either
315 cytokine would depend on cytoplasmic PRRs. Many single stranded RNA viruses,

316 including NDV and influenza [31], have been found to activate retinoic acid inducible
317 gene-I (RIG-I). RIG-I bound to viral RNA interacts with the adaptor protein called
318 mitochondrial antiviral-signaling protein (MAVS), triggering the events leading to IFN
319 synthesis. To determine the role of MAVS activation in the production of each IFN type,
320 we made use of MAVS-/- mice, available on the C57BL/6 background. WT and MAVS
321 deficient animals were inoculated with NDV, and both IFN-α and IFN-λ levels were
322 determined by ELISA of BALs collected 24 hours post-infection. As expected, there was
323 no induction of either cytokine in the absence of MAVS, demonstrating that the events
324 triggered by NDV recognition are dependent on cytoplasmic pattern recognition pathways
325 in both cell types (Fig 14).
326
327 Since our studies of IFN-λ induction by IAV suggested that pDCs are the predominant
328 type III IFN producing cell population *in vivo,* we wished to determine which signaling
329 pathways were triggered by this infection. Several reports have previously shown that
330 pDC recognition of the influenza genomic ssRNA by the TLR7 endosomal pathway that
331 signals through the protein myeloid differentiation primary response 88 protein (MyD88)
332 [32-34] results in robust type I IFN expression. Based on our finding that pDCs are also
333 the major source of type III IFNs in response to IAV infection, we suspected that this
334 pathway was also required for optimal IFN-λ production. To test this assumption, MAVS-
335 /- mice on the C57BL6 background were infected with the WSN and PR8 strains of IAV,
336 and IFN-λ protein levels were measured in BALs. We saw no reduction in IFN-λ
337 expression following PR8 infection of MAVS-/- mice at 24, 48 and 72 hours post infection
338 (Fig 15A), but a ~ 40% reduction following WSN infection at 48 hours post infection,

consistent with data from our pDC depletion study. Conversely, in the absence of MyD88 (Fig 15B), a more significant reduction in IFN-λ was seen in the BALs of WSN-infected mice. Taken together, our data show that while both pathways can contribute to IFN-λ production following IAV infection, the major contribution is pDC derived, particularly for the PR8 strain of IAV.

We further explored this IAV strain dependence *ex vivo* using WT murine tracheal epithelial cells (mTEC) cultured at an air-liquid interface on transwell filters. IFN-λ protein levels in culture supernatants from virus infected mTECs showed robust production by NDV or WSN infected cultures, but no detectable IFN-λ following PR8 infection (Fig 16). This result is consistent with our inability to detect epithelial IFN-λ production following PR8 infection *in vivo*, and the absence of a requirement for functional MAVS protein.

Plasmacytoid DC production of IFN-λ requires type I IFN signaling

We and others have observed no significant difference in the resistance of wild type and IFNAR-/- mice to IAV infection [22, 35]. In the absence of the type I IFN pathway, IFN-λ production is sufficient to inhibit virus replication and spread. Assuming that pDCs were a major source of this cytokine, GFP expression was assayed in pDCs isolated from the lungs of PR8-infected *Ifnl2*$^{gfp/gfp}$ mice on WT or IFNAR-/- 129SvEv strain backgrounds. In this experiment, pDCs from IAV-infected *Ifnl2*$^{gfp/gfp}$ reporter mice with intact type I IFN signaling expressed GFP, but strongly reduced expression was detected in pDCs from IFNAR deficient *Ifnl2*$^{gfp/gfp}$ animals (Fig 17A). *In vitro* WSN infection of FLT3L cultured pDCs derived from bone marrow of wild type or IFNAR-/- mice produced the same result,

with ELISA-detectable amounts of IFN-λ protein found only in medium from IAV-infected IFNAR$^{+/+}$ pDC cultures.

Plasmacytoid DCs are unique for their constitutive expression of interferon regulatory factor 7 (IRF7), a transcription factor essential for the induction of IFN-α genes [36]. IRF7 has also been implicated as a driver for IFN-λ transcriptional activation [37] [38]. Given the importance of IRF7 in the induction of IFN genes, we looked to see whether IRF7 levels were altered in the absence of IFNAR. As shown in Figure 17C, qPCR analysis demonstrated a substantial reduction in basal levels of IRF7 mRNA in IFNAR-/- pDCs. Since IRF7 is itself an ISG, we conclude that pDCs require some level of tonic activation of the type I IFN signaling pathway to maintain sufficient IRF7 for type III IFN induction in response to IAV infection. Interestingly, there was no decrease in GFP+ epithelial cells in NDV-infected IFNAR-/- IFN-λ reporter mice (Fig 18), supporting our conclusion that type I IFN-dependent maintenance of IRF7 levels in pDCs is essential for optimal type III IFN induction by IAV.

Discussion

Since the discovery of type III IFNs in 2003 [3] [4] and the demonstration that identical sets of ISGs are induced by type I and type III IFNs in sensitive cells [39, 40], many groups have sought to determine whether these cytokines play a unique role in antiviral immunity. It has been found that type I and type III IFN receptors are differentially expressed by different cell types. While most immune cells in mouse and man are IFN-α responsive, only human pDCs, neutrophils and B cells have been found to consistently respond to IFN-λ [11, 30, 41, 42]. Until recently it was thought that all epithelial cells respond to both

385 IFN-α/β and IFN-λ, but recent *in vivo* studies have demonstrated that intestinal epithelial
386 cells become IFN-α insensitive soon after birth, and respond only to IFN-λ *in situ* [19].
387 These observations point to distinct roles for type I and type III IFNs in innate immune
388 responses, determined primarily by the responsiveness and sensitivity of specific cell
389 types to IFN-α/β and IFN-λ, but also by the availability of their ligands.

390 Our goal in generating an IFN-λ reporter mouse was to investigate the source of this
391 cytokine as a viral infection of an epithelial surface progressed. This was done by
392 replacing the *IFNL2* coding sequence with *eGFP*, a reporter gene whose expression is
393 then regulated by the *IFNL2* promoter, UTR regions and other elements surrounding the
394 *IFNL2* gene. Our first aim was to determine the extent to which GFP expression correlated
395 with IFN-λ production by various cell types. *In vitro* virus infection of both epithelial and
396 dendritic cells derived from the reporter mice induced GFP expression, and only GFP+
397 cells were found to express IFN-λ transcripts. Equally important were studies to confirm
398 GFP and IFN-λ co-expression *in vivo*. Lauterbach *et al*. [17] had previously demonstrated
399 that splenic CD8α DCs were the major producers of IFN-λ following systemic treatment
400 with poly(I:C), a TLR3 ligand, and we established that GFP expression in the IFN-λ
401 reporter mouse was limited to that cell type (Fig 3) following i.v. administration of poly(I:C).
402 We next asked whether GFP expression by the *Ifnl2*$^{gfp/gfp}$ reporter mouse would
403 recapitulate the pattern of IFN-λ expression previously described for heterologous
404 rotavirus infection. Hernandez *et al*. [43] reported that IFN-λ transcripts were present only
405 in CD45- EPCAM+ intestinal epithelial cells, but not expressed by cells isolated from
406 lamina propria during RV infection. We repeated this study in WT and IFN-λ reporter
407 suckling mice, harvesting tissue at the time point corresponding to maximal IFN

responsiveness post-infection. Elevated, and equivalent, levels of IFN-λ were detected in intestinal homogenates from both strains following infection, with GFP expression detectable only in the epithelial compartment (Fig 6). We concluded from these results that GFP expression is an accurate indicator of IFN-λ expression in this reporter mouse strain and, importantly, that IFN-λ expression levels are equivalent in WT and *Ifnl2*$^{gfp/gfp}$ mice where production of IFN-λ3 protein compensates for the lack of the functional *IFNL2* gene.

The mucosal surfaces of the gastrointestinal and respiratory tracts are major portals of virus entry, and infection of these organs induces the secretion of both type I and type III IFNs [19, 22, 25, 43]. While both IFN types contribute to an effective antiviral response, receptor distribution suggests that type III IFNs have a primary role in protecting epithelial cells and that IFN-λ production is therefore crucial to an effective antiviral response at these barrier surfaces. While it is established that epithelial cells are the major IFN-λ producers during RNA virus infection of intestinal epithelial cells [10, 19], we wished to determine whether this was also a feature of respiratory virus infection. Using an IFN-α reporter mouse, Kamagai *et al.* [5] had demonstrated that IFN-α production following NDV infection was limited to alveolar macrophages. This was a surprising and important finding as it had been widely understood that essentially all cell types produced type I IFNs in response to NDV infection *in vitro*. As many respiratory virus infections result in the production of both type I IFNs and type III IFNs, we wished to determine whether alveolar macrophages were the source of both cytokines, or whether these cytokines were produced by different cell types in response to the same viral pathogen.

NDV infection of the IFN-λ reporter mouse resulted in GFP expression only by EPCAM+ epithelial cells as measured by flow cytometry and immunohistochemistry, and *in situ* hybridization studies detected IFN-λ transcripts only in bronchial epithelial cells of NDV-infected animals. This result is consistent with other published studies that have described IFN-λ production by mouse and human airway epithelial cells in response to respiratory viruses *in vivo* [23, 44-47]. Like Kumagai *et al*., we observed IFN-α mRNA induction in alveolar macrophages isolated from the lungs of NDV-infected animals, but no IFN-λ transcripts were detected in these cells. Therefore, NDV simultaneously induces both type I and type III IFNs upon respiratory infection, but each IFN type is produced by a different cell type.

Cellular recognition of RNA viruses generally occurs through recognition of viral genomes or viral transcripts by TLRs and RIG-I-like receptors, which signal through MyD88 and MAVS, respectively, to induce the expression of IFNs. TLRs are generally expressed by hematopoietic cells and RIG-I-like receptors by epithelial cells, although TLR3 expression at the apical surface of polarized murine and human tracheal epithelial cell cultures has been demonstrated [29]. Our results in MAVS-/- mice indicate that both IFN-α and IFN-λ production following NDV infection requires MAVS activation, but we do not yet understand how activation of this pathway by the same virus leads to production of one or the other IFN type in a cell type dependent manner. The most likely explanation is suggested by work showing that MAVS is located on the surface of mitochondria and peroxisomes [48], and further, that signaling via MAVS on peroxisomes induces type III, but not type I IFN production [9]. Preferential IFN-λ synthesis following MAVS activation was found to depend upon the relative abundance

of peroxisomes in a given cell type, and polarization of intestinal epithelial cells resulted in increased numbers of these organelles. While these data predict a shift in the relative levels of type I and type III IFN production by different cell types, the complete absence of IFN-λ synthesis by alveolar macrophages in infected animals was unexpected. Further investigation is required to understand this compartmentalization of IFN production that we observe *in vivo*.

As NDV infection is abortive in mammalian cells [49], it was of interest to repeat these studies using IAV, which replicates and causes disease in the murine host. Based on our NDV data, and published reports which suggested that infected epithelial cells were the primary source of type III IFNs in IAV infection [30, 45], we expected our influenza studies to confirm this conclusion, but this was not the case. By all approaches taken it appeared that, for IAV infection, the bulk of IFN-λ was produced by pDCs rather than the respiratory epithelium. When pDC-depleted mice were infected with IAV, there was a 60% reduction in BAL levels of both type I and type III IFNs. Infection of bone marrow chimeras generated by the transfer of *Ifnl-/-* bone marrow into WT mice showed a similar decrease in type III IFN induction by IAV. In our study, ~ 40% of the IFN-λ induced by IAV was from non-pDC sources, but this was dependent on virus strain. While GFP+ pDCs were detected using either the PR8 or WSN strains of IAV, only in WSN infections was epithelial IFN-λ synthesis detected *in vivo* or *ex vivo*. The conclusion that type III IFN synthesis induced by PR8 came primarily from pDCs was further supported by studies in MAVS-/- animals which showed no impact on IFN-λ levels in the absence of this pathway in PR8 infection.

476 Also of interest was our finding that IFN-λ production by IAV-exposed pDCs is type I
477 IFN dependent. Our data suggest that the tonic signaling through the type I IFN receptor
478 may be required to maintain the elevated basal levels of IRF7 which is a hallmark of this
479 cell type [50]. While this result was unexpected, it is consistent with the observation that
480 human subjects with a deficiency of IRF7 expression are more likely to experience life-
481 threatening infections of influenza [51] as well as SARS-CoV-2 [52]. As both type I and
482 type III IFNs are known to play a role in protection from respiratory viruses, this
483 observation is further support of the hypothesis that pDCs are the major source of both
484 of these cytokines during IAV infection. The demonstration that both IFN-α and IFN-λ
485 are produced by IAV-exposed human pDCs [11] also supports this possibility.
486 In summary, we have used an IFN-λ reporter mouse model to determine the source of
487 type III IFNs in two mouse models of respiratory virus infection. For NDV, type I and
488 type III IFNs are simultaneously induced through the engagement of the same virus
489 sensing pathway, but from two distinct cell types with respiratory epithelium as the sole
490 source of IFN-λ. In IAV infection, pDCs appear to produce the bulk of type III IFN, and
491 its production by this cell type requires type I IFN signaling. This study suggests that
492 IFN induction by viruses *in vivo* is pathogen specific, as is the source of these cytokines.
493
494 **Methods**

495 **Generation of the IFN-λ Reporter Mouse**

496 Generation of the IFN-λ reporter mouse was carried out by ingenious Targeting
497 Laboratory (www.genetargeting.com). The targeting vector was constructed using an
498 11 kb region of a C57BL/6 BAC clone (RP23: 24B20), containing the *Ifnl2* locus, sub-
499 cloned into the pSP72 backbone vector (Promega). A GFP/FRT-flanked neomycin

cassette was inserted into the BAC subclone using Red/ET recombineering technology, resulting in the complete replacement of the *IFNλ2* coding region of exons 1-5 (including intron sequences), with a long homology arm extending approximately 6.91 kb 5' to the site of the cassette insertion and a short homology arm that extends approximately 2.68 kb 3' to the site of the cassette insertion. The GFP-Neomycin targeting vector was linearized by Not I enzymatic digestion and electroporated into BA1 (C57B/6 x 129SvEv) hybrid embryonic stem cells. G418 resistant ES cell clones expanded for PCR analysis to identify homologous recombinants. Clones found to carry the GFP transgene were sequenced to confirm insertion, sequence fidelity, the genome/5' cassette junction and the genome/3' cassette junction. Southern blot analysis of positive clones was carried out using ApaI digestion of PCR products hybridized with a probe targeted against the 5'external region. Targeted BA1 hybrid embryonic stem cells were microinjected into C57BL/6 blastocysts and resulting chimeras with a high percentage agouti coat color were mated to C57BL/6 FLP mice to remove the neomycin cassette. Tail DNA from pups with agouti or black coat color was analyzed by PCR to confirm presence of transgene. Animals heterozygous for the *Ifnl2*$^{+/gfp}$ allele were backcrossed onto the 129SvEv background for 10 generations, then bred to produce homozygous animals. Genotyping was carried out by two PCR reactions: One reaction using Primer A (5'-CAGAGCTGGAAACTCAGAGCC-3') and Primer B (5'-GACCGAGTCTGAGACCCACAAG-3') and another reaction using Primer C (5'-CAGAGCTGGAAACTCAGAGCC-3') and Primer B. Thermocycler conditions for those reactions were as follows: 95° C for 15 minutes, followed by 35 cycles of (94° C for 45 minutes, 65° C for 1 minute, and 72° C for 1.5 minutes), with an end step of 72° C for 5

minutes. The amplicon generated by Primers A and B, which encompasses the *Ifnl2* or *gfp* region, was then digested with the NcoI restriction endonuclease. NcoI treatment of the wildtype allele yields a 1100 bp band and a 700 bp band, while digestion of the amplicon containing the *Ifnl2*$^{+/gfp}$ allele, which lacks NcoI restriction sites, yields a single 1110 bp band.

Additional Mice

Mice on the 129SvEv background lacking the type I IFN receptor (IFNAR-/-) were originally derived by Michel Aguet [53] and strain matched controls were purchased from Taconic Farms. MAVS-/- and MYD88-/- mice on the C57BL/6 background were obtained from Jackson Labs. Mx2-Luc Mx2 luciferase reporter mice were obtained from Hansjörg Hauser and Mario Köster [21]. Generation of the IFN-λ-/- mice, lacking both the IFN-λ2 and -λ3, sequences is described in supplemental figure 2. All mice were maintained under specific pathogen-free conditions in the vivarium of Rutgers-New Jersey Medical School.

Cell culture

Bone-marrow derived FLT3-ligand dendritic cell cultures were generated from the bone marrow of IFN-λ reporter mice, *ifnl-/-* mice and WT controls. Bone marrow from femurs and tibia of 6-10 week old mice was washed, depleted of red cells with ACK lysis buffer, and cultured in RPMI+10% FBS containing 100 ng/mL human FLT3-ligand (Peprotech), 50 μM β-mercaptoethanol (Sigma), penicillin (100 IU/ml.) and streptomycin (100 μg/ml) at a cell density of 3x10^6 cells/ml for 7 – 8 days.

546

547 For preparation of kidney epithelial cells, kidney capsules were removed, renal
548 parenchyma was minced into 1 mm^3 pieces and digested with collagenase IV
549 (Worthington) at 37°C for 30 min. Following red blood cell lysis, digested tissue was
550 pressed through a100 μM, then a 40 μM cell strainer, and the recovered cells were
551 washed and then plated in DMEM/HamsF12 with 10% FBS. After 1-2 hours of
552 incubation, non-adherent cells were collected and plated on collagen-coated dishes.
553 Cells were allowed to reach 70% confluence prior to virus infection.

554

555 Murine tracheal epithelial cells were derived from WT or IFN-λ reporter mice at 6 to 10
556 weeks of age following the procedures outlined by You et al. [54].

557

558 **Poly I:C Treatment and Splenic DC Analysis**

559 6-10 week old IFN-λ reporter mice were injected intravenously with sterile PBS or 100
560 μg polyI:C (InVivoGen). Splenocytes were harvested 6 hours after treatment, incubated
561 with anti-mouse CD32/Fc-Block (BD Pharmingen) for 10 minutes at 4°C, then stained
562 with the following antibodies: anti-mouse CD45-BUV395 (BD Horizon), anti-mouse
563 CD3-APC Cy7 (BioLegend), anti-mouse CD11c-APC (eBioscience), anti-mouse CD11b-
564 PerCP Cy5.5 (ebioscience), anti-mouse CD8α-V450 (BD Horizon), and anti-mouse
565 Siglec-H-PE (eBioscience) antibodies. Analysis was carried out using the LSRII (BD
566 Biosciences) flow cytometer.

567

568

569

570 **Virus infection and assay**

571 Six-day-old suckling mice were infected with $4x10^6$ PFU of the simian RRV strain by
572 oral gavage. Intestines were harvested 24 hours post-infection. These were either
573 formalin fixed or homogenized in medium for virus quantitation. RRV quantitation was
574 done using a focus forming assay as previously described [19].

575 Six-10 week old mice, under isoflurane anesthesia, were infected intranasally with 10^7
576 PFU of NDV (Hitchner B1 strain) in 50 µl of PBS. Mice were euthanized 24 hours post-
577 infection for collection of bronchoalveolar lavage fluid and lung tissue.

578 *In vitro* infection of primary kidney epithelial cells was carried out at a multiplicity of
579 infection (MOI) of 2 and 20. Infections were done with RRV, the Hitchner B1 strain of
580 NDV, the A2 strain of respiratory syncytial virus (RSV), and the WSN strain of influenza
581 A virus (IAV).

582 A/PR?8?34 and A/WSN/33 influenza viruses were grown in embryonated chicken eggs.
583 Allantoic fluid was assay for infectious viral particles by focus forming assay on MDCK
584 cells. Serial dilutions of allantoic fluid were prepared and incubated on MDCK cells at
585 37°C, in 5% $C0_2$ for 24 hours. Cells were then fixed in phosphate-buffered formalin, and
586 viral plaques were visualized by incubating fixed cells with polyclonal rabbit anti-IAV
587 serum (US Biologicals), followed by HRP-conjugated secondary antibodies for
588 visualization of plaques via a colorimetric assay.

589

590

591

Ethics statement

All mouse studies were approved by the Institutional Animal Care and Use Committees of Rutgers-New Jersey Medical School (protocols 999900760 and 13009C0316), performed in compliance with relevant institutional policies, local, state, and federal laws, and conducted following National Research Council Guide for the Care and Use of Laboratory Animals, Eighth Edition.

In vivo luciferase detection

Six-day old Mx2-Luc mice were injected intraperitoneally with D-Luciferin (15 µg per pup), (Perkin Elmer), anesthetized with isoflurane, and imaged using the IVIS-200 Vivo Vision system (Caliper). Gray-scale images followed by bioluminescent images were then acquired and superimposed using the Living Image software (Caliper). Bioluminescent images represent luciferase signal intensity, with red as highest and blue as lowest, respectively. Regions of interest with detectable luciferase activity were measured quantitatively as relative light units (RLUs) at 3, 6, 12, 24, 48, 72, and 96 hours post-RRV infection.

Immunostaining

Harvested tissues were fixed in 10% neutral buffered formalin, and submitted for processing and paraffin embedding. Deparaffinized sections underwent antigen retrieval and were subsequently blocked with Superblock (ScyTek) for 5 minutes at room temperature, washed in wash buffer (PBS+0.05% Tween) and then stained using anti-NDV antibodies (US Biological), anti-RRV antibodies (Meridian), anti-eGFP (Life

Technologies) antibodies or anti-IAV antibodies (US Biological)overnight at 4°C. The following day, slides were washed in wash buffer and stained using anti-DyLight488 (Abcam) or anti-DyLight564 (Abcam) secondary antibodies for 1 hour at room temperature in the dark, washed in wash buffer, and incubated with DAPI for 6 minutes. After washing in distilled water, mounting medium (Vectashield) was applied, and slides were coverslipped. Images were obtained using an Axiovert 200M inverted fluorescence microscope (Zeiss) using the AxioVision LE64 software (Zeiss).

Lung digestion and flow cytometry analysis

Perfused lungs were finely minced and digested in 5 mL of a 1.78mg/mL Collagenase IV (Worthington) solution in PBS (with Ca^{2+}, Mg^{2+}) for 45 minutes at 37°C. Lung digests were further dissociated by passage through a 20G needle, then filtration through a 100 µm filter. ACK lysis buffer was used to remove red blood cells, and remaining cell suspension was washed twice with PBS. Lung cell suspensions were first blocked with anti-CD32/Fc-Block (BD Pharmingen) for 10 minutes at 4°C, then stained with cocktail of primary antibodies including: anti-mouse CD45-BUV395 (BD Horizon), anti-mouse EPCAM-PECy7 (BioLegend), anti-mouse Ly6G-Alexa Fluor 700 (BioLegend), anti-mouse F4/80-APC (BioLegend), anti-mouse CD11c-PerCPCy5.5 (BioLegend), anti-mouse CD11b-APC-Cy7 (BioLegend), and anti-mouse Siglec F-PE (BD Pharmingen). Cells were then washed in FACS buffer (PBS+2% FBS and sodium azide), resuspended in FACS Buffer containing DAPI, and analyzed using an LSRII flow cytometer (BD Biosciences). Sorting of stained cell populations was carried out on an Aria II Cell sorter (BD Biosciences).

638

639 **Plasmacytoid DC depletion**

640 Mice were injected i.p. with 500 μg of anti-PDCA1 or Rat IgG 24 and 48 hours before
641 IAV infection. Mice were sacrificed 24 hours post-infection to collect BALS, and blood
642 and spleens were collected to stain for pDC surface marker (CD11c+, CD11b-, B220+,
643 PDCA1+).

644

645 ***In situ* hybridization**

646 *In situ* detection of IFN-λ transcripts was carried out using the RNA Scope© HD 2.5
647 Detection Reagent-Red kit (Advanced Cell Technologies) according to manufacturer's
648 instructions. Briefly, formalin-fixed, paraffin-embedded tissue sections were heated at
649 60°C for 1 hour, deparaffinized in xylene and 100% alcohol, and incubated with
650 hydrogen peroxide for 10 minutes at room temperature. Antigen retrieval was then
651 carried out for 1 hour in RNA Scope antigen retrieval buffer, and slides were washed in
652 distilled water and 100% ethanol, and then left to dry overnight. The following day,
653 slides were washed in RNA Scope proprietary wash buffer and incubated in protease-
654 plus buffer, washed again, and then incubated with mouse IFNλ2/3 DNA probes
655 (Advanced Cell Technologies), followed by a series of RNA Scope adaptor probes,
656 streptavidin-HRP, and chromogen solution to visualize IFN-λ transcripts. Slides were
657 counterstained with 50% Lillie Mayer's hematoxylin (American Master Tech Scientific
658 Inc).

659

660

661 **RNA isolation and qRT-PCR**

662 RNA from cells was obtained using the RNA Easy Kit (Qiagen) incorporating the
663 DNAse I step to remove contaminating genomic DNA. cDNA was synthesized using
664 iScript cDNA Synthesis kit (Biorad) using 10 ng RNA, with 10% of the cDNA product
665 used for qPCR analysis. The following primer pairs were used to carry out qPCR
666 reactions in a CFX96 Real Time System (BioRad) using SYBR Green (BioRad):
667 IFNλ2/3 Forward 5'-TCAAGC ACCTCTTCTCGATGG-3'
668 IFNλ2/3 Reverse 5'-AGCTGCAGGCCTTCAAAAAG-3'
669 IFNα Forward 5'-TCTGATGCAGCAGGTGGG-3'
670 IFNα Reverse 5'-AGGGCTCTCCAGACTTCTGCTCTG-3'
671 18s rRNA Forward 5'-GTAACCCGTTGAACCCCATT-3'
672 18s rRNA Reverse 5'-CCATCCAATCGGTAGTAGCG-3'
673 eGFP Forward 5'-GACGTAAACGGCCACAAGTT-3'
674 eGFP Reverse 5'-ATG CCGTTCTTCTGCTTGT-3'
675 Thermocycler conditions were set with the following parameters for amplification of
676 IFNλ2/3 transcripts: 95°C for 3 minutes, followed by 40 cycles of 95°C for 10 seconds
677 and a gene-specific annealing temperature for 30 seconds. Gene-specific annealing
678 temperatures for IFNλ2/3, IFNα, eGFP were 58.4°C, 61.3°C, and 58.4°C, respectively.
679 18s rRNA qPCR reactions using the same annealing temperature as the target gene of
680 interest were carried out simultaneously. Relative normalized expression was
681 determined by normalizing amplification of IFN-λ, IFN-α, or eGFP expression to 18s
682 rRNA levels by the ΔΔCt method [PMID 11846609].
683

Data analysis

Data were analyzed using GraphPad Prism version 7 (graphPad Software). Mean and SEM were calculated by the same.

Acknowledgments

Authors are thankful to Hansjörg Hauser and Mario Köster for Mx2-luciferase reporter mice. Histology and Imaging were done with the assistance of the New Jersey Medical Histology and Imaging Core Laboratory. This work was funded by grants from the National Institutes of Health: R21 AI073597 (JED), U01 AI082994 (JED) and R01 AI104264 (SVK and JED).

Literature Cited

1. Isaacs A, Lindenmann J. Virus interference. I. The interferon. Proc R Soc Lond B Biol Sci. 1957;147(927):258-67. PubMed PMID: 13465720.
2. Isaacs A, Lindenmann J, Valentine RC. Virus interference. II. Some properties of interferon. Proc R Soc Lond B Biol Sci. 1957;147(927):268-73. PubMed PMID: 13465721.
3. Kotenko SV, Gallagher G, Baurin VV, Lewis-Antes A, Shen M, Shah NK, et al. IFN-lambdas mediate antiviral protection through a distinct class II cytokine receptor complex. Nat Immunol. 2003;4(1):69-77. Epub 2002/12/17. doi: 10.1038/ni875. PubMed PMID: 12483210.
4. Sheppard P, Kindsvogel W, Xu W, Henderson K, Schlutsmeyer S, Whitmore TE, et al. IL-28, IL-29 and their class II cytokine receptor IL-28R. Nat Immunol. 2003;4(1):63-8. Epub 2002/12/07. doi: 10.1038/ni873. PubMed PMID: 12469119.
5. Kumagai Y, Takeuchi O, Kato H, Kumar H, Matsui K, Morii E, et al. Alveolar macrophages are the primary interferon-alpha producer in pulmonary infection with

RNA viruses. Immunity. 2007;27(2):240-52. doi: 10.1016/j.immuni.2007.07.013. PubMed PMID: 17723216.

6. Goritzka M, Makris S, Kausar F, Durant LR, Pereira C, Kumagai Y, et al. Alveolar macrophage-derived type I interferons orchestrate innate immunity to RSV through recruitment of antiviral monocytes. J Exp Med. 2015;212(5):699-714. doi: 10.1084/jem.20140825. PubMed PMID: 25897172; PubMed Central PMCID: PMCPMC4419339.

7. Kotenko SV, Durbin JE. Contribution of type III interferons to antiviral immunity: location, location, location. J Biol Chem. 2017;292(18):7295-303. Epub 2017/03/16. doi: 10.1074/jbc.R117.777102. PubMed PMID: 28289095; PubMed Central PMCID: PMCPMC5418032.

8. Lazear HM, Nice TJ, Diamond MS. Interferon-lambda: Immune Functions at Barrier Surfaces and Beyond. Immunity. 2015;43(1):15-28. Epub 2015/07/23. doi: 10.1016/j.immuni.2015.07.001. PubMed PMID: 26200010; PubMed Central PMCID: PMCPMC4527169.

9. Odendall C, Dixit E, Stavru F, Bierne H, Franz KM, Durbin AF, et al. Diverse intracellular pathogens activate type III interferon expression from peroxisomes. Nat Immunol. 2014;15(8):717-26. doi: 10.1038/ni.2915. PubMed PMID: 24952503; PubMed Central PMCID: PMCPMC4106986.

10. Mahlakoiv T, Hernandez P, Gronke K, Diefenbach A, Staeheli P. Leukocyte-derived IFN-alpha/beta and epithelial IFN-lambda constitute a compartmentalized mucosal defense system that restricts enteric virus infections. PLoS Pathog. 2015;11(4):e1004782. doi: 10.1371/journal.ppat.1004782. PubMed PMID: 25849543; PubMed Central PMCID: PMCPMC4388470.

11. Yin Z, Dai J, Deng J, Sheikh F, Natalia M, Shih T, et al. Type III IFNs are produced by and stimulate human plasmacytoid dendritic cells. J Immunol. 2012;189(6):2735-45. doi: 10.4049/jimmunol.1102038. PubMed PMID: 22891284; PubMed Central PMCID: PMCPMC3579503.

12. Brehm G, Kirchner H. Analysis of the interferons induced in mice in vivo and in macrophages in vitro by Newcastle disease virus and by polyinosinic-polycytidylic acid. J Interferon Res. 1986;6(1):21-8. PubMed PMID: 2422299.

13. Wimmers F, Subedi N, van Buuringen N, Heister D, Vivie J, Beeren-Reinieren I, et al. Single-cell analysis reveals that stochasticity and paracrine signaling control interferon-alpha production by plasmacytoid dendritic cells. Nat Commun. 2018;9(1):3317. Epub 2018/08/22. doi: 10.1038/s41467-018-05784-3. PubMed PMID: 30127440; PubMed Central PMCID: PMCPMC6102223.

14. Ank N, West H, Bartholdy C, Eriksson K, Thomsen AR, Paludan SR. Lambda interferon (IFN-lambda), a type III IFN, is induced by viruses and IFNs and displays potent antiviral activity against select virus infections in vivo. J Virol. 2006;80(9):4501-9. Epub 2006/04/14. doi: 10.1128/JVI.80.9.4501-4509.2006. PubMed PMID: 16611910; PubMed Central PMCID: PMCPMC1472004.

15. Ank N, Iversen MB, Bartholdy C, Staeheli P, Hartmann R, Jensen UB, et al. An important role for type III interferon (IFN-lambda/IL-28) in TLR-induced antiviral activity. J Immunol. 2008;180(4):2474-85. PubMed PMID: 18250457.

16. Coccia EM, Severa M, Giacomini E, Monneron D, Remoli ME, Julkunen I, et al. Viral infection and Toll-like receptor agonists induce a differential expression of type I

763 and lambda interferons in human plasmacytoid and monocyte-derived dendritic cells.
764 Eur J Immunol. 2004;34(3):796-805. Epub 2004/03/03. doi: 10.1002/eji.200324610.
765 PubMed PMID: 14991609.
766 17. Lauterbach H, Bathke B, Gilles S, Traidl-Hoffmann C, Luber CA, Fejer G, et al.
767 Mouse CD8alpha+ DCs and human BDCA3+ DCs are major producers of IFN-lambda
768 in response to poly IC. J Exp Med. 2010;207(12):2703-17. doi: 10.1084/jem.20092720.
769 PubMed PMID: 20975040; PubMed Central PMCID: PMCPMC2989774.
770 18. Crawford SE, Ramani S, Tate JE, Parashar UD, Svensson L, Hagbom M, et al.
771 Rotavirus infection. Nat Rev Dis Primers. 2017;3:17083. Epub 2017/11/10. doi:
772 10.1038/nrdp.2017.83. PubMed PMID: 29119972.
773 19. Lin JD, Feng N, Sen A, Balan M, Tseng HC, McElrath C, et al. Distinct Roles of
774 Type I and Type III Interferons in Intestinal Immunity to Homologous and Heterologous
775 Rotavirus Infections. PLoS Pathog. 2016;12(4):e1005600. doi:
776 10.1371/journal.ppat.1005600. PubMed PMID: 27128797; PubMed Central PMCID:
777 PMCPMC4851417.
778 20. Pott J, Mahlakoiv T, Mordstein M, Duerr CU, Michiels T, Stockinger S, et al. IFN-
779 lambda determines the intestinal epithelial antiviral host defense. Proc Natl Acad Sci U
780 S A. 2011;108(19):7944-9. Epub 2011/04/27. doi: 10.1073/pnas.1100552108. PubMed
781 PMID: 21518880; PubMed Central PMCID: PMCPMC3093475.
782 21. Pulverer JE, Rand U, Lienenklaus S, Kugel D, Zietara N, Kochs G, et al.
783 Temporal and spatial resolution of type I and III interferon responses in vivo. J Virol.
784 2010;84(17):8626-38. Epub 2010/06/25. doi: 10.1128/JVI.00303-10. PubMed PMID:
785 20573823; PubMed Central PMCID: PMCPMC2919002.
786 22. Jewell NA, Cline T, Mertz SE, Smirnov SV, Flano E, Schindler C, et al. Lambda
787 interferon is the predominant interferon induced by influenza A virus infection in vivo. J
788 Virol. 2010;84(21):11515-22. doi: 10.1128/JVI.01703-09. PubMed PMID: 20739515;
789 PubMed Central PMCID: PMCPMC2953143.
790 23. Khaitov MR, Laza-Stanca V, Edwards MR, Walton RP, Rohde G, Contoli M, et al.
791 Respiratory virus induction of alpha-, beta- and lambda-interferons in bronchial epithelial
792 cells and peripheral blood mononuclear cells. Allergy. 2009;64(3):375-86. Epub
793 2009/01/30. doi: 10.1111/j.1398-9995.2008.01826.x. PubMed PMID: 19175599.
794 24. Mordstein M, Neugebauer E, Ditt V, Jessen B, Rieger T, Falcone V, et al.
795 Lambda interferon renders epithelial cells of the respiratory and gastrointestinal tracts
796 resistant to viral infections. J Virol. 2010;84(11):5670-7. Epub 2010/03/26. doi:
797 10.1128/JVI.00272-10. PubMed PMID: 20335250; PubMed Central PMCID:
798 PMCPMC2876583.
799 25. Mahlakoiv T, Ritz D, Mordstein M, DeDiego ML, Enjuanes L, Muller MA, et al.
800 Combined action of type I and type III interferon restricts initial replication of severe
801 acute respiratory syndrome coronavirus in the lung but fails to inhibit systemic virus
802 spread. J Gen Virol. 2012;93(Pt 12):2601-5. doi: 10.1099/vir.0.046284-0. PubMed
803 PMID: 22956738.
804 26. de Maeyer-Guignard J, de Maeyer E. Effect of antilymphocytic serum on
805 circulating interferon in mice as a function of the inducer. Nat New Biol.
806 1971;229(7):212-4. Epub 1971/02/17. PubMed PMID: 4325471.
807 27. Honda K, Sakaguchi S, Nakajima C, Watanabe A, Yanai H, Matsumoto M, et al.
808 Selective contribution of IFN-alpha/beta signaling to the maturation of dendritic cells

809 induced by double-stranded RNA or viral infection. Proc Natl Acad Sci U S A.
810 2003;100(19):10872-7. Epub 2003/09/10. doi: 10.1073/pnas.1934678100. PubMed
811 PMID: 12960379; PubMed Central PMCID: PMCPMC196895.
812 28. Hillyer P, Mane VP, Schramm LM, Puig M, Verthelyi D, Chen A, et al. Expression
813 profiles of human interferon-alpha and interferon-lambda subtypes are ligand- and cell-
814 dependent. Immunol Cell Biol. 2012;90(8):774-83. Epub 2012/01/18. doi:
815 10.1038/icb.2011.109. PubMed PMID: 22249201; PubMed Central PMCID:
816 PMCPMC3442264.
817 29. Ioannidis I, Ye F, McNally B, Willette M, Flano E. Toll-like receptor expression
818 and induction of type I and type III interferons in primary airway epithelial cells. J Virol.
819 2013;87(6):3261-70. doi: 10.1128/JVI.01956-12. PubMed PMID: 23302870; PubMed
820 Central PMCID: PMCPMC3592129.
821 30. Galani IE, Triantafyllia V, Eleminiadou EE, Koltsida O, Stavropoulos A,
822 Manioudaki M, et al. Interferon-lambda Mediates Non-redundant Front-Line Antiviral
823 Protection against Influenza Virus Infection without Compromising Host Fitness.
824 Immunity. 2017;46(5):875-90 e6. Epub 2017/05/18. doi: 10.1016/j.immuni.2017.04.025.
825 PubMed PMID: 28514692.
826 31. Kato H, Takeuchi O, Sato S, Yoneyama M, Yamamoto M, Matsui K, et al.
827 Differential roles of MDA5 and RIG-I helicases in the recognition of RNA viruses.
828 Nature. 2006;441(7089):101-5. Epub 2006/04/21. doi: 10.1038/nature04734. PubMed
829 PMID: 16625202.
830 32. Lund JM, Alexopoulou L, Sato A, Karow M, Adams NC, Gale NW, et al.
831 Recognition of single-stranded RNA viruses by Toll-like receptor 7. Proc Natl Acad Sci
832 U S A. 2004;101(15):5598-603. Epub 2004/03/23. doi: 10.1073/pnas.0400937101.
833 PubMed PMID: 15034168; PubMed Central PMCID: PMCPMC397437.
834 33. Diebold SS, Kaisho T, Hemmi H, Akira S, Reis e Sousa C. Innate antiviral
835 responses by means of TLR7-mediated recognition of single-stranded RNA. Science.
836 2004;303(5663):1529-31. Epub 2004/02/21. doi: 10.1126/science.1093616. PubMed
837 PMID: 14976261.
838 34. Koyama S, Ishii KJ, Kumar H, Tanimoto T, Coban C, Uematsu S, et al.
839 Differential role of TLR- and RLR-signaling in the immune responses to influenza A
840 virus infection and vaccination. J Immunol. 2007;179(7):4711-20. Epub 2007/09/20. doi:
841 10.4049/jimmunol.179.7.4711. PubMed PMID: 17878370.
842 35. Mordstein M, Kochs G, Dumoutier L, Renauld JC, Paludan SR, Klucher K, et al.
843 Interferon-lambda contributes to innate immunity of mice against influenza A virus but
844 not against hepatotropic viruses. PLoS Pathog. 2008;4(9):e1000151. Epub 2008/09/13.
845 doi: 10.1371/journal.ppat.1000151. PubMed PMID: 18787692; PubMed Central PMCID:
846 PMCPMC2522277.
847 36. Izaguirre A, Barnes BJ, Amrute S, Yeow WS, Megjugorac N, Dai J, et al.
848 Comparative analysis of IRF and IFN-alpha expression in human plasmacytoid and
849 monocyte-derived dendritic cells. J Leukoc Biol. 2003;74(6):1125-38. Epub 2003/09/10.
850 doi: 10.1189/jlb.0603255. PubMed PMID: 12960254.
851 37. Osterlund PI, Pietila TE, Veckman V, Kotenko SV, Julkunen I. IFN regulatory
852 factor family members differentially regulate the expression of type III IFN (IFN-lambda)
853 genes. J Immunol. 2007;179(6):3434-42. Epub 2007/09/06. doi:
854 10.4049/jimmunol.179.6.3434. PubMed PMID: 17785777.

855 38. Hatesuer B, Hoang HT, Riese P, Trittel S, Gerhauser I, Elbahesh H, et al.
856 Deletion of Irf3 and Irf7 Genes in Mice Results in Altered Interferon Pathway Activation
857 and Granulocyte-Dominated Inflammatory Responses to Influenza A Infection. J Innate
858 Immun. 2017;9(2):145-61. Epub 2016/11/05. doi: 10.1159/000450705. PubMed PMID:
859 27811478; PubMed Central PMCID: PMCPMC6738875.
860 39. Doyle SE, Schreckhise H, Khuu-Duong K, Henderson K, Rosler R, Storey H, et
861 al. Interleukin-29 uses a type 1 interferon-like program to promote antiviral responses in
862 human hepatocytes. Hepatology. 2006;44(4):896-906. Epub 2006/09/29. doi:
863 10.1002/hep.21312. PubMed PMID: 17006906.
864 40. Marcello T, Grakoui A, Barba-Spaeth G, Machlin ES, Kotenko SV, MacDonald
865 MR, et al. Interferons alpha and lambda inhibit hepatitis C virus replication with distinct
866 signal transduction and gene regulation kinetics. Gastroenterology. 2006;131(6):1887-
867 98. Epub 2006/11/08. doi: 10.1053/j.gastro.2006.09.052. PubMed PMID: 17087946.
868 41. Broggi A, Tan Y, Granucci F, Zanoni I. IFN-lambda suppresses intestinal
869 inflammation by non-translational regulation of neutrophil function. Nat Immunol.
870 2017;18(10):1084-93. Epub 2017/08/29. doi: 10.1038/ni.3821. PubMed PMID:
871 28846084; PubMed Central PMCID: PMCPMC5701513.
872 42. Espinosa V, Dutta O, McElrath C, Du P, Chang YJ, Cicciarelli B, et al. Type III
873 interferon is a critical regulator of innate antifungal immunity. Sci Immunol. 2017;2(16).
874 Epub 2017/10/08. doi: 10.1126/sciimmunol.aan5357. PubMed PMID: 28986419.
875 43. Hernandez PP, Mahlakoiv T, Yang I, Schwierzeck V, Nguyen N, Guendel F, et al.
876 Interferon-lambda and interleukin 22 act synergistically for the induction of interferon-
877 stimulated genes and control of rotavirus infection. Nat Immunol. 2015;16(7):698-707.
878 doi: 10.1038/ni.3180. PubMed PMID: 26006013; PubMed Central PMCID:
879 PMCPMC4589158.
880 44. Okabayashi T, Kojima T, Masaki T, Yokota S, Imaizumi T, Tsutsumi H, et al.
881 Type-III interferon, not type-I, is the predominant interferon induced by respiratory
882 viruses in nasal epithelial cells. Virus Res. 2011;160(1-2):360-6. doi:
883 10.1016/j.virusres.2011.07.011. PubMed PMID: 21816185.
884 45. Crotta S, Davidson S, Mahlakoiv T, Desmet CJ, Buckwalter MR, Albert ML, et al.
885 Type I and type III interferons drive redundant amplification loops to induce a
886 transcriptional signature in influenza-infected airway epithelia. PLoS Pathog.
887 2013;9(11):e1003773. Epub 2013/11/28. doi: 10.1371/journal.ppat.1003773. PubMed
888 PMID: 24278020; PubMed Central PMCID: PMCPMC3836735.
889 46. Bosco A, Wiehler S, Proud D. Interferon regulatory factor 7 regulates airway
890 epithelial cell responses to human rhinovirus infection. BMC Genomics. 2016;17:76.
891 Epub 2016/01/27. doi: 10.1186/s12864-016-2405-z. PubMed PMID: 26810609; PubMed
892 Central PMCID: PMCPMC4727386.
893 47. Fox JM, Crabtree JM, Sage LK, Tompkins SM, Tripp RA. Interferon Lambda
894 Upregulates IDO1 Expression in Respiratory Epithelial Cells After Influenza Virus
895 Infection. J Interferon Cytokine Res. 2015;35(7):554-62. doi: 10.1089/jir.2014.0052.
896 PubMed PMID: 25756191; PubMed Central PMCID: PMCPMC4507134.
897 48. Dixit E, Boulant S, Zhang Y, Lee AS, Odendall C, Shum B, et al. Peroxisomes
898 are signaling platforms for antiviral innate immunity. Cell. 2010;141(4):668-81. doi:
899 10.1016/j.cell.2010.04.018. PubMed PMID: 20451243; PubMed Central PMCID:
900 PMCPMC3670185.

49. Mentkevich LM, Orlova TG. Multiplication of Newcastle disease virus strains and interferon production in the mouse, an animal naturally insusceptible to this infection. Acta Virol. 1966;10(3):226-9. Epub 1966/05/01. PubMed PMID: 4381333.
50. Honda K, Yanai H, Negishi H, Asagiri M, Sato M, Mizutani T, et al. IRF-7 is the master regulator of type-I interferon-dependent immune responses. Nature. 2005;434(7034):772-7. Epub 2005/04/01. doi: 10.1038/nature03464. PubMed PMID: 15800576.
51. Ciancanelli MJ, Huang SX, Luthra P, Garner H, Itan Y, Volpi S, et al. Infectious disease. Life-threatening influenza and impaired interferon amplification in human IRF7 deficiency. Science. 2015;348(6233):448-53. Epub 2015/03/31. doi: 10.1126/science.aaa1578. PubMed PMID: 25814066; PubMed Central PMCID: PMCPMC4431581.
52. Zhang Q, Bastard P, Liu Z, Le Pen J, Moncada-Velez M, Chen J, et al. Inborn errors of type I IFN immunity in patients with life-threatening COVID-19. Science. 2020;370(6515). Epub 2020/09/26. doi: 10.1126/science.abd4570. PubMed PMID: 32972995; PubMed Central PMCID: PMCPMC7857407.
53. Muller U, Steinhoff U, Reis LF, Hemmi S, Pavlovic J, Zinkernagel RM, et al. Functional role of type I and type II interferons in antiviral defense. Science. 1994;264(5167):1918-21. Epub 1994/06/24. doi: 10.1126/science.8009221. PubMed PMID: 8009221.
54. You Y, Brody SL. Culture and differentiation of mouse tracheal epithelial cells. Methods Mol Biol. 2013;945:123-43. Epub 2012/10/26. doi: 10.1007/978-1-62703-125-7_9. PubMed PMID: 23097105.

Figure Legends

Figure 1. Generating the IFN-λ Reporter Mouse.

(A) The targeting vector carrying *eGFP* and *Neo* genes was inserted into the *Ifnl2* locus by homologous recombination, resulting in complete replacement of the *Ifnl2* coding region with the *eGfp* and *Neo* genes. Excision of the *Neo* gene was carried out by crossing mice carrying the targeted allele with Flipase mice, resulting in deletion of the *Neo* gene and generation of the *Ifnl2*$^{+/gfp}$ allele. (B) PCR products generated with primers shown in (A), and digested with Nco1, yielded unique banding patterns for tail DNA obtained from WT 129 SvEv mice (+/+), heterozygous *Ifnl2*$^{+/gfp}$ (+/-), and homozygous *Ifnl2*$^{gfp/gfp}$ IFN-λ reporter animals. (C) Pictured are phase contrast and GFP immunofluorescence images (200x) of uninfected or NDV-infected, FLT3L cultured, bone marrow derived DCs from *Ifnl2*$^{gfp/gfp}$ mice. Images are representative of three independent experiments. (D) NDV-infected FLT3L cultured, bone marrow derived DCs were cell sorted into GFP+ and GFP- fractions that were then assayed by qRT-PCR for the presence of GFP and IFN-λ3 transcripts. Data are representative of two independent experiments. (E) Flow cytometry dot plots show GFP expression in cultures of primary kidney epithelial cells (gated as EPCAM+ cells) derived from *Ifnl2*$^{gfp/gfp}$ mice that were mock-infected or infected with Newcastle disease virus (NDV), rhesus rotavirus (RRV), respiratory syncytial virus (RSV), or influenza A virus (IAV) at the indicated MOIs for 24 hrs. Data are representative of two independent experiments.

948 **Figure 2. CD8α DCs are the predominant IFN-λ-producing cells in spleens of mice**
949 **treated intravenously with poly I:C.**
950 (A) Flow cytometry analysis of splenic populations from IFN-λ reporter mice mock-
951 treated (left) or i.v. treated with poly I:C (right) for 6 hrs. Cells were gated on CD11c
952 while simultaneously excluding CD3+ cells to exclude T cells. Dendritic cell populations
953 were then identified as follows: pDCs (CD11c+/Siglec-H+/CD11b-); CD8α DCs (Siglec-
954 H-/CD11b-/CD8α+); cDCs (Siglec-H-/CD11b+/CD11c+). (B) Mean percentages, with
955 SEM, of GFP+ cells in populations shown in (A). Data are representative of two
956 independent experiments.
957
958 **Figure 3. Epithelial cells are the predominant IFN-λ-producing cell population in**
959 **the small intestine in response to RRV.**
960 **(**A) Interferon responses of 6-day old, RRV-infected Mx2-Luciferase transgenic mice
961 were quantitated by IVIS at the indicated timepoints. (B) Graphical representation of
962 mean luciferase activity values and SEM from two independent experiments. (C) ELISA
963 measurements of IFN-λ protein in homogenates of intestinal tissue harvested from 6-
964 day old WT C57BL/6 pups, 24 hours after RRV infection. (D) Comparison of RRV viral
965 titers, measured by fluorescent-focus assay, in the small intestine of 6-day old WT 129
966 SvEV mice and IFN-λ reporter mice 3 days post-RRV infection. Data are pooled from
967 two independent experiments. (E) Images of formalin-fixed paraffin-embedded (FFPE)
968 small intestinal tissue sections from mock- or RRV-infected IFN-λ reporter pups, and
969 RRV-infected WT pups, were captured 24 hours post-infection. Sections were probed

970 with anti-GFP antibodies (green), anti-RRV sera (red) and DAPI (blue) and visualized by
971 fluorescence microscopy. Images are representative of three independent experiments.
972
973 **Figure 4. Epithelial cells are the predominant IFN-λ producers in response to NDV**
974 **infection in vivo.**
975 (A) GFP expression was assayed by flow cytometry of cells obtained from collagenase-
976 digested lungs of IFN-λ reporter mice which were mock-infected or infected intranasally
977 with NDV for 24 hrs. Epithelial cells were defined as CD45-, EPCAM+. WT 129SvEV
978 mice were included as controls for GFP expression, gating in the same manner. (B)
979 Graphical representation of mean percentage of GFP+ epithelial cells from each
980 treatment cohort. Error bars represent SEM. (C) IFN-λ protein levels in BALs harvested
981 at 24 hours from mock-infected or NDV-infected reporter mice were determined by
982 ELISA. (D) Lung sections from uninfected IFN-λ reporter mice, and NDV-infected WT
983 and NDV-infected IFN-λ reporter mice were stained with anti-GFP antibodies (green),
984 anti-NDV antibodies (red), and DAPI (blue). Data are representative of three
985 independent experiments.
986
987 **Figure 5. WT and IFN-λ reporter mice produce similar levels of type I and type III**
988 **IFNs following NDV infection *in vivo*.**
989 (A) Levels of IFN-λ and (B) IFN-α proteins in BAL samples from WT or IFN-λ reporter
990 mice 24 hours after mock- or NDV (10^7 pfu) infection were quantified by ELISA. Data
991 are pooled from two independent experiments.
992

Figure 6. Alveolar macrophages and other myeloid cells do not produce IFN-λ during NDV infections *in vivo*. GFP expression was assayed by flow cytometry analysis of cells obtained from collagenase-digested lungs of mock-infected or NDV-infected IFN-λ reporter mice or infected WT animals. Cell populations are defined as follows: alveolar macrophages (F4/80+,Ly6G-, SiglecF+, CD11c+), neutrophils (F4/80-, LY6G+), monocyte-derived macrophages (F4/80+, Ly6G-, SiglecF-, CD11c-) , and eosinophils (F4/80+, Ly6G-, SiglecF+, CD11c-). Data is representative of three independent experiments.

Figure 7. Kinetics of IFN-λ induction by NDV *in vivo*

GFP expression by (A) alveolar macrophages and (B) respiratory epithelial cells obtained from the lungs of mock- or NDV-infected IFN-λ reporter mice was assayed by flow cytometry. Samples were obtained at post-infection intervals of 10, 24, and 48 hours. (C) Graphical representation of mean % of GFP+ cells at each time point. Data are representative of two independent experiments.

Figure 8. Distinct cell sources of IFN-α and IFN-λ *in vivo*.

(A) Cell sorting strategy for isolation of alveolar macrophage and epithelial cell populations from collagenase-digested lungs obtained from mock- or NDV-infected WT mice 24 hours post-infection mice. Isolated populations of epithelial cells (CD45-/EPCAM+) and alveolar macrophages (as CD45+/F4/80+/Siglec F+/CD11c+) are indicated with an asterisk. (B) RNA harvested from FACS-sorted epithelial cells and alveolar macrophages and used to synthesize cDNA for detection of endogenous

IFNλ2/3 transcripts by qPCR. qPCR detection of endogenous pan-IFNα transcripts (non-IFNα4) was also performed on FACS-sorted (C) alveolar macrophages and (D) epithelial cells. Expression is shown normalized to 18s rRNA. Data are pooled from two independent experiments. (E) *In situ* hybridization assays to detect endogenous IFN-λ transcripts were carried out on FFPE lung sections from NDV-infected WT and IFN-λ reporter mice at the 24 hour time point using probes specific for IFN-λ2/3 transcripts (seen in red). Images are representative of two independent experiments.

Figure 9. NDV infection of alveolar macrophages *in vitro*.

(A) Sorting strategy for the isolation of alveolar macrophages from collagenase-digested lungs of uninfected WT mice. Isolated alveolar macrophages were then infected with NDV *in vitro* at the indicated MOIs. Supernatants and RNA samples were collected at 24 hours post-infection. (B) cDNA was synthesized from the RNA of mock- or NDV-infected cells and used to detect *Ifnl2/3* expression by qPCR. RNA isolated from cells stably transfected with a construct expressing FLAG-tagged murine IFN-λ2 (FL-mIFN-λ2 cells) was included as a positive control. (C) Levels of IFN-λ and IFN-α proteins secreted into the medium by cultured alveolar macrophages were determined by ELISA. Culture medium from FL-mIFN-λ2 cells was used as a positive control. Data are representative of two independent experiments

Figure 10. Plasmacytoid dendritic cells are the major producers of IFN-λ during IAV infections *in vivo*

(A) BAL samples collected from mock-infected or IAV-infected IFN-λ reporter mice were assayed by ELISA for the measurement of IFN-λ protein in airways. (B) Representative flow cytometry plots evaluating GFP expression specifically in epithelial cells, characterized as EPCAM+ cells (initially gated from DAPI-/CD45- and single cell populations), from single-cell suspensions of collagenase-digested lungs from mock-infected and IAV-infected (WSN; 10^6 PFUs, 48 hrs) IFN-λ reporter mice or WT 129 SvEv controls. (C) Flow cytometry plots demonstrating gating scheme of pDCs from the lungs of the same mice as in (A). From initial gating of DAPI-/CD45+ and single cells, pDCs were gated as CD11c+/CD11b-, B220+/PDCA1+, from which GFP expression was assessed. Graphs on the right represent SEM of %GFP+ pDCs, and number of pDCs from each cohort. Data are pooled from three independent experiments. (D) qPCR analysis of IFN-λ and IFN-α transcripts in epithelial cells and pDCs that were FACS-sorted from the single cell suspension of collagenase-digested lungs from of mock-infected and IAV (WSN)-infected WT 129 SvEv mice (10^5 PFUs, 48 hrs). Data are representative of two independent experiments. (E) Formalin fixed lung tissue sections from mock-infected or IAV-infected (10^6 PFUs WSN) IFN-λ reporter mice, harvested at the indicated time points, were stained with IFN-λ oligonucleotide probes to detect *ifnl* RNA transcripts. Data are representative of two independent experiments.

Figure 11. **Minimal IFN-λ expression by epithelial cells during IAV infections is not due to a NS1-mediated inhibition**

Representative flow cytometry plots showing GFP expression from (A) epithelial cells (gated from DAPI-/CD45-/EPCAM+) and (B) pDCs (gated from DAPI-

/CD45+/CD11c+/CD11b-/B220+/PDCA1+) from wildtype 129 SvEv mice and IFN-λ reporter mice mock-infected or infected with 10^4 PFUs of either IAV (PR8) or IAVΔNS1 (PR8ΔNS1) for 48 hrs. (C) SEM of %GFP epithelial cells and pDCs from each cohort.

Figure 12. The hematopoietic compartment is the source of the bulk of IFN-λ protein produced during IAV infection.

Bone marrow chimera mice, generated by reconstituting lethally irradiated wildtype C57BL6/J mice with bone marrow from either wildtype C57BL6/J mice or *ifnl*$^{-/-}$ mice, were infected with 10^5 PFUs IAV (WSN) for 48 hrs, at which point BAL samples were harvested and assayed for IFN-λ protein by ELISA. The graph represents the mean and SEM of IFN-λ protein levels measured from each cohort. Data were pooled from two independent experiments

Figure 13. Depletion of pDCs during IAV infections in vivo results in significant reduction of both Type I and Type III IFNs

(A) Representative flow cytometry plots show pDC populations in the spleen and blood of IAV-infected mice (10^6 PFUs WSN strain; 24 hrs post-infection) that were treated with the pDC-depleting antibody (anti-PDCA1) or the Rat IgG isotype 24 hours and 48 hours prior to IAV infection. Graphs on the right show mean percentages, and SEM, of pDCs in the spleen and blood of each indicated cohort**.** (B) BALs were harvested 24 hours post-IAV infection for IFN-λ protein measurements. Graphs represent data from two independent experiments

Figure 14. IFN-λ induction by NDV is MAVS-dependent

(A) IFN-λ and (B) IFN-α protein levels were measured by ELISA in BALs of mock-infected or NDV-infected (24 hrs, 10^7 PFUs) WT and $MAVS^{-/-}$ mice on the C57BL/6 strain background. Differences in IFN-λ levels between WT and $MAVS^{-/-}$ mice were statistically significant as determined by student t test (P = 0.0474). No IFN-α protein was detectable in mock-infected or NDV-infected $MAVS^{-/-}$ animals. Data were pooled from two independent experiments

Figure 15. Contribution of MAVS and MyD88 signaling in IFN-λ induction during IAV infections is dependent on IAV strain

(A) IFN-λ protein levels were measured by ELISA from BALs of IAV-infected (10^6 PFUs PR8) wildtype C57BL/6J mice or $MAVS^{-/-}$ mice at the indicated time points. (B) IFN-λ protein levels measured by ELISA from BALs of IAV-infected (10^5 PFUs WSN) wildtype C57BL/6J mice, $MyD88^{-/-}$, or $MAVS^{-/-}$ mice at 48 hours post-infection. Graphs represent the mean and SEM of IFN-λ protein measured from the BALs of each cohort. Data from each figure were pooled from two independent experiments.

Figure 16. Murine tracheal epithelial cells produce IFN-λ in response to WSN but not to PR8 infection

Murine tracheal epithelial cultures were infected apically, at an MOI of 1, with NDV, WSN, PR8 or UV-inactivated PR8 for 24 hours. Supernatants were then assayed by ELISA for IFN-λ protein.

Figure 17. IFN-λ production by pDCs during IAV infection is dependent on type I IFN signaling

(A) Flow cytometry plots showing GFP expression in pDCs (DAPI-/CD45+/CD11c^{+}/CD11b^{-}/B220^{+}/PDCA1^{+}) from the lungs of IFNAR+/+ or IFNAR$^{-/-}$ IFN-λ reporter mice, or 129 SvEv mice, mock-infected or IAV-infected (PR8 10^{6} PFUs, for 72 hrs). The graph on the right represents mean and SEM of %GFP+ cells from each cohort. (B) Supernatants from mock-infected or IAV-infected (WSN; MOI=1) WT and IFNAR$^{-/-}$ FLT3L-cultured bone-marrow derived pDCs were collected 24 hours post-infection, and assayed for IFN-λ protein by ELISA. (**C)** qPCR measurements comparing basal levels of IRF7 mRNA expression between WT and IFNAR$^{-/-}$ bone-marrow derived pDCs. Data were pooled from two independent experiments.

Figure 18. IFN-λ production during NDV infection is type I IFN-independent

GFP expression was assayed by flow cytometry of cells obtained from collagenase-digested lungs of 129 SvEv WT and IFNAR-/- IFN-λ reporter mice which were mock-infected, or infected intranasally with NDV for 24 hrs. Epithelial cells were defined as CD45-, EPCAM+. WT 129SvEV mice were included as controls for GFP expression, gating in the same manner. No significant differences in GFP expression were seen between IFN-λ reporter animals on the WT or IFNAR-/- backgrounds.

Supplemental Figure 1. Viral loads are equivalent in WT and reporter mice

Cohorts of 6-10 week old WT 129 SvEv mice or strain-matched IFN-λ reporter mice were infected with 10^{2} PFUs of IAV (WSN). Viral titers from the lungs were assayed by

immunofocus assay from lung homogenates collected at 72 hrs post-infection. The graph represents SEM of PFUs quantified for each cohort. This is experiment was performed twice.

Supplemental Figure 2. Generation of *ifnl-/-* mice

The mouse genome contains two functional IFN-λ genes, the IFN-λ2 and IFN-λ3 genes, which are juxtaposed in a head-to-head orientation on chromosome 7. Guidance RNAs (gRNAs) were designed to target sequences flanking these genes, and the CRISPR/Cas9 technology was used to generate mice lacking both IFN-λ genes, to create an IFN-λ2/3 knock-out (KO) strain. The selected IFN-λ2/3 KO strain contains 19,803 base pair deletion (from 28,506,772 to 28,526,525 nucleotide positions; NCBI GRCm38.p4) that removed the entire IFN-λ2 and IFN-λ3 genes including their promoters and 3'UTR, and replaced these with ATAACTTCGTATAGCATA sequence.

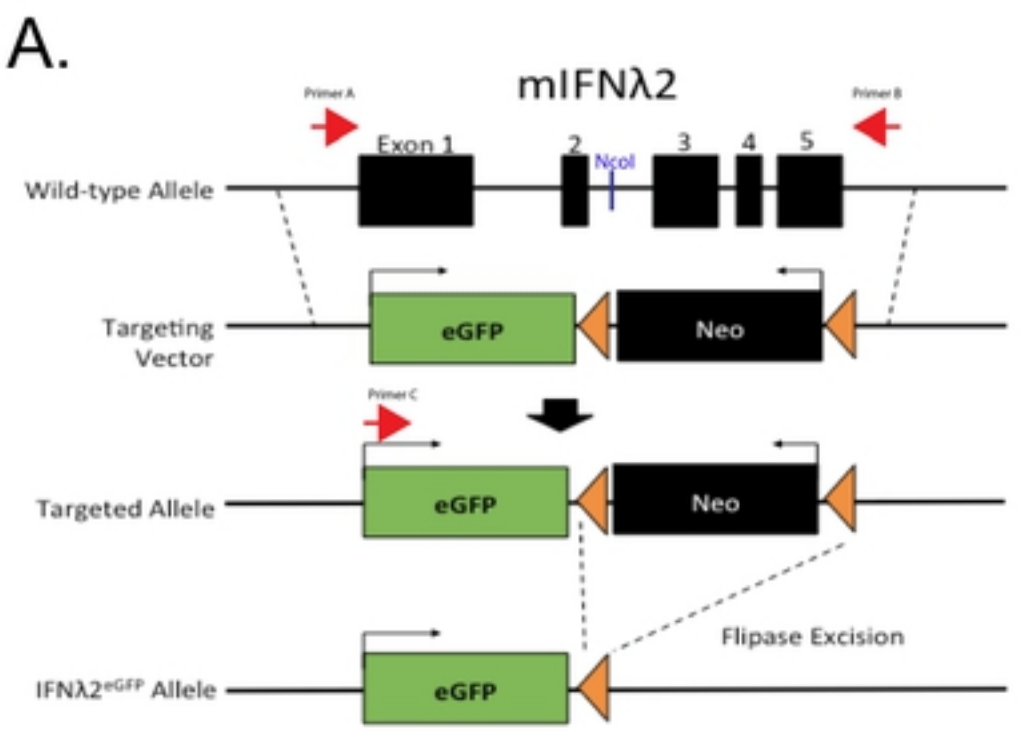

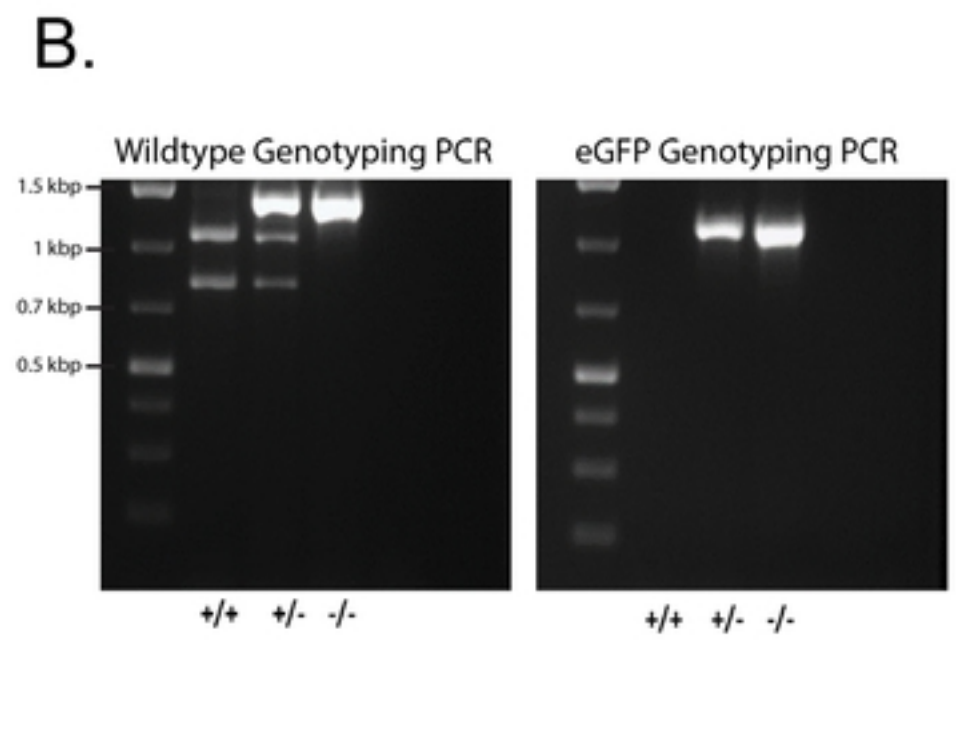

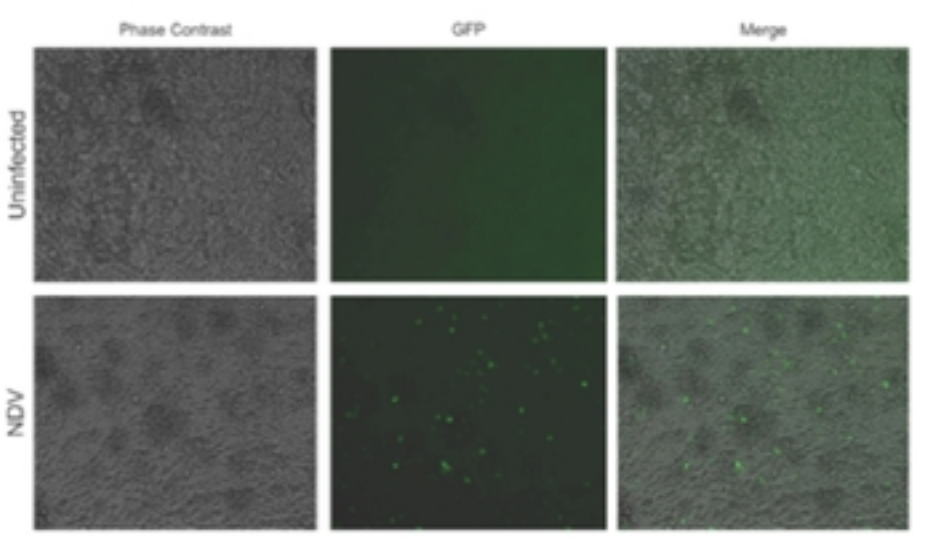

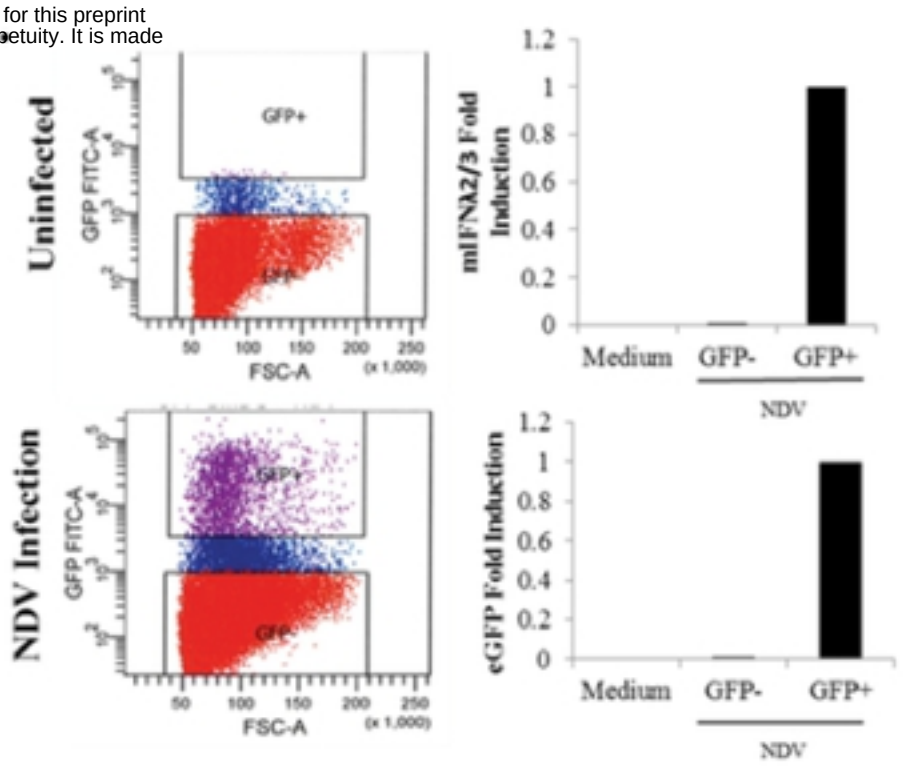

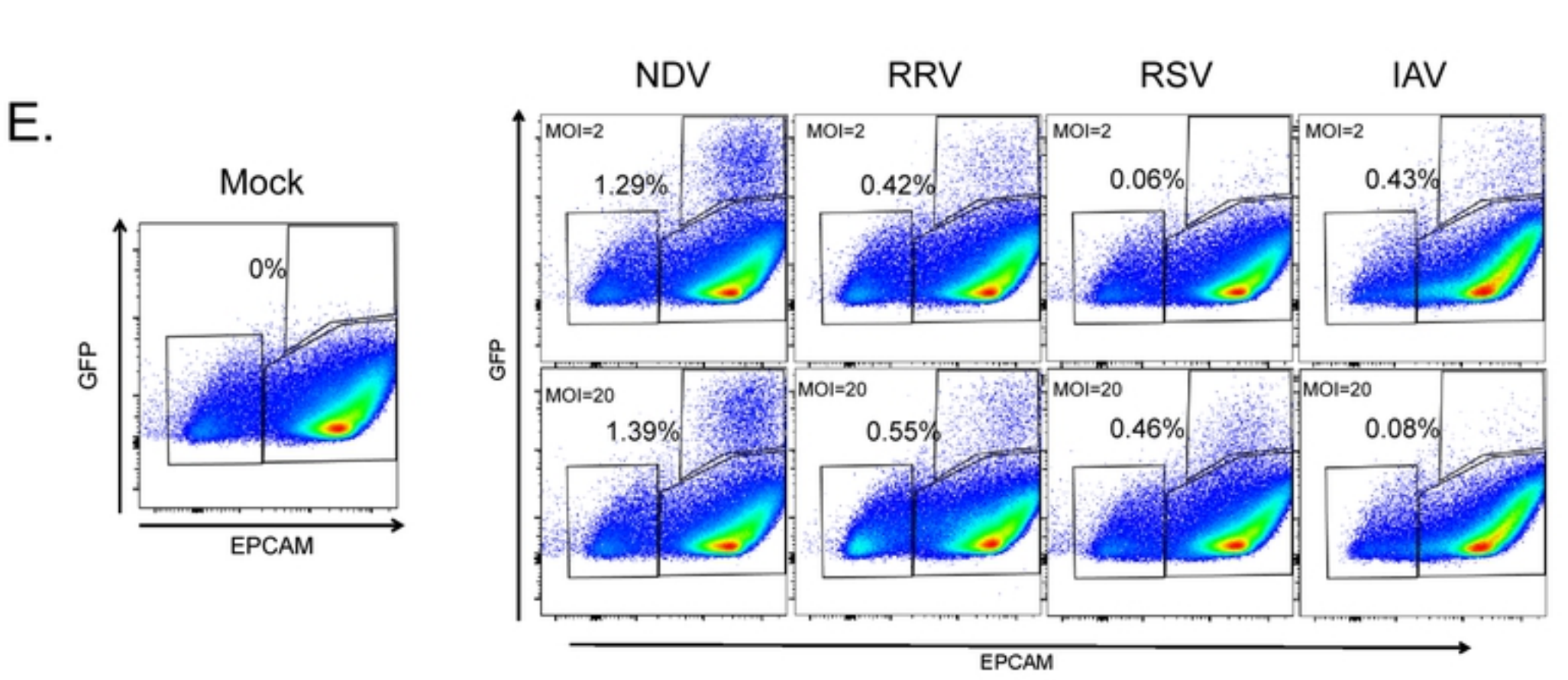

Figure

A.

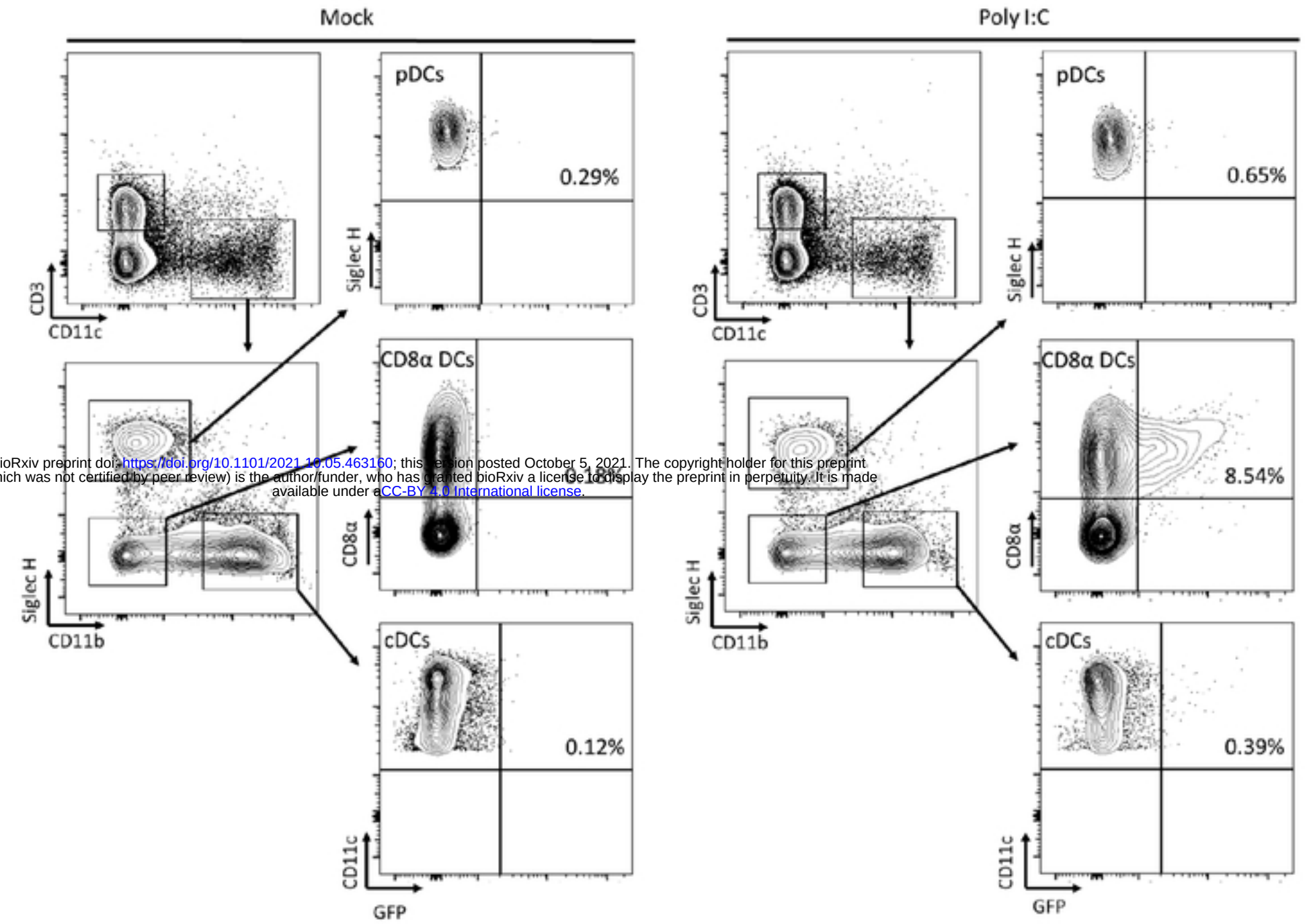

B.

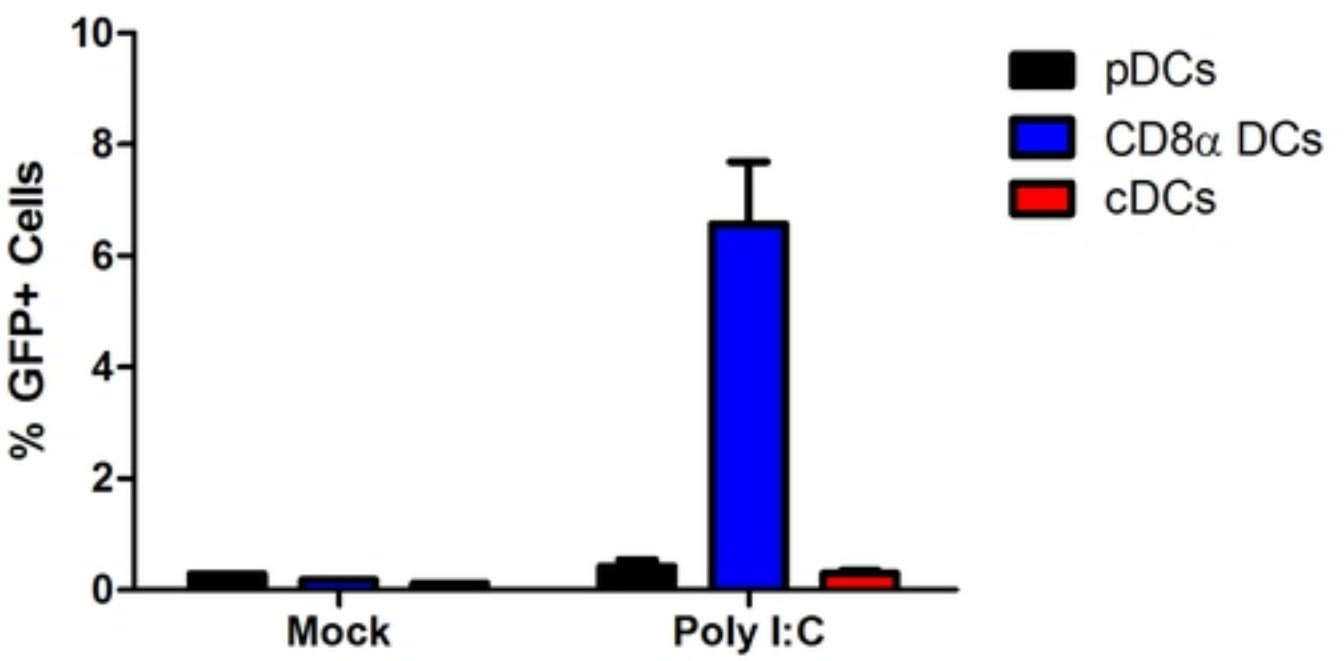

Figure

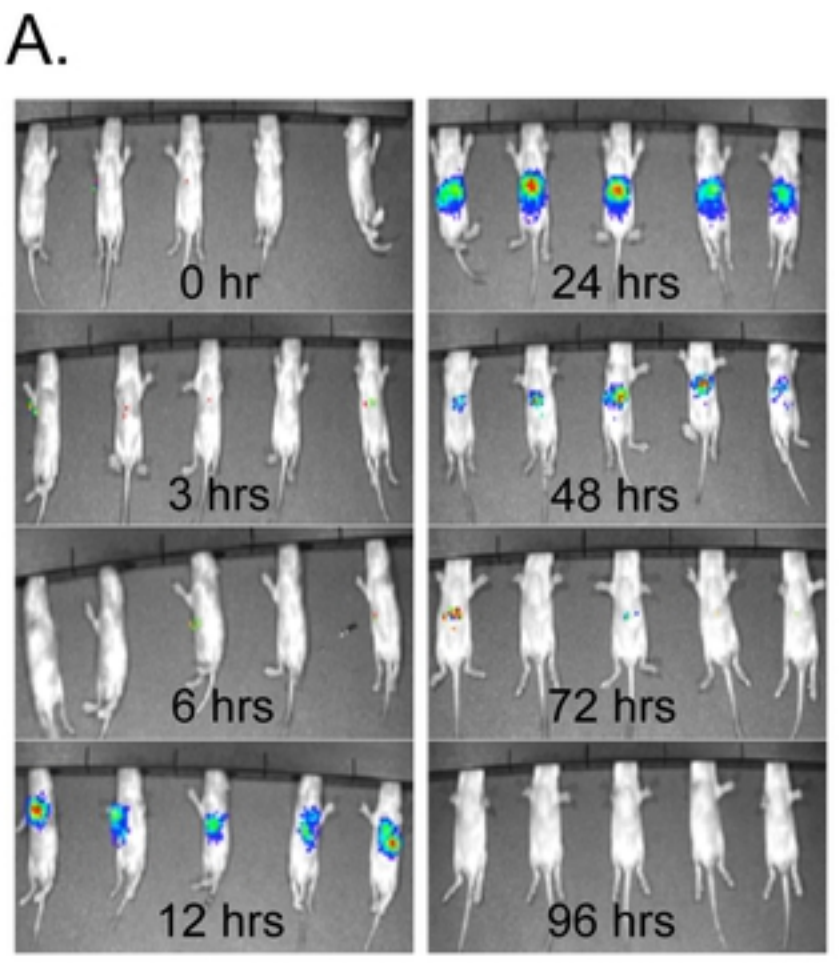

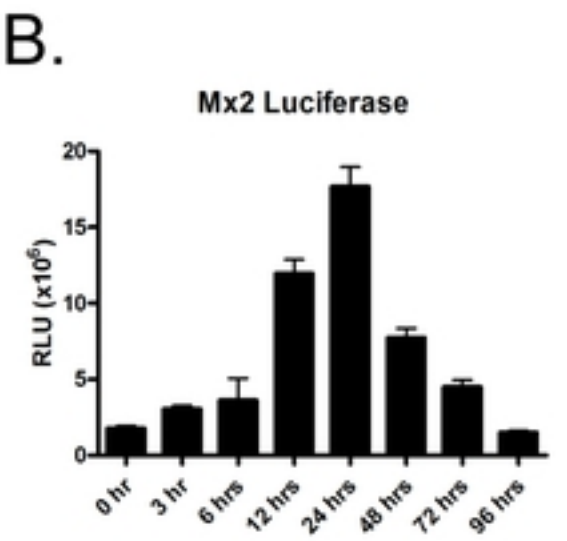

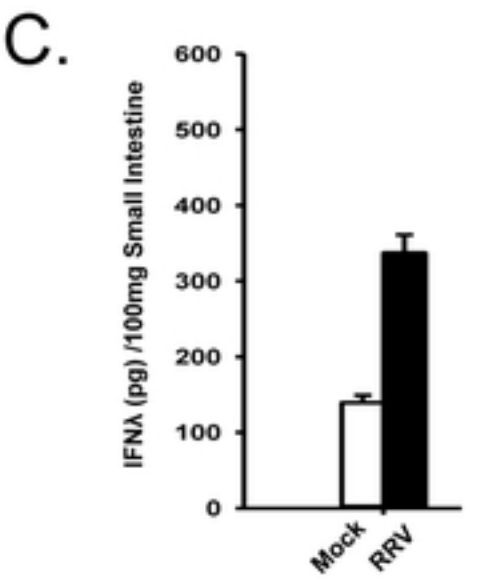

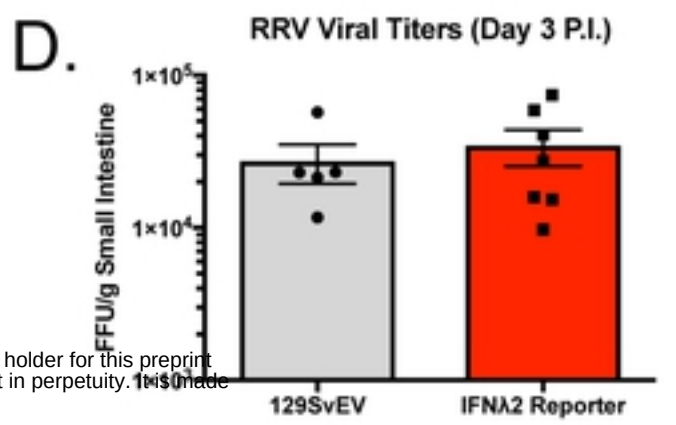

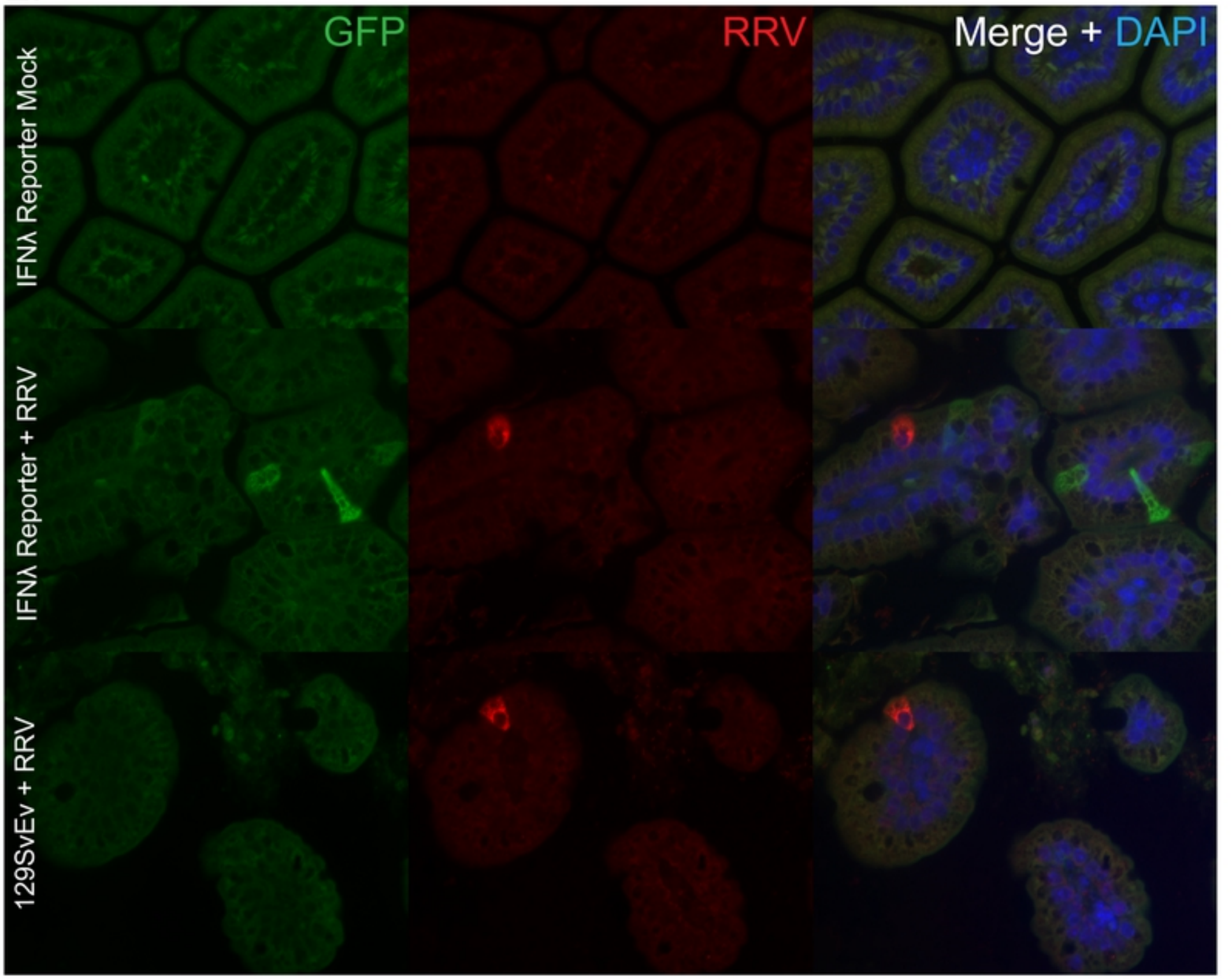

Figure

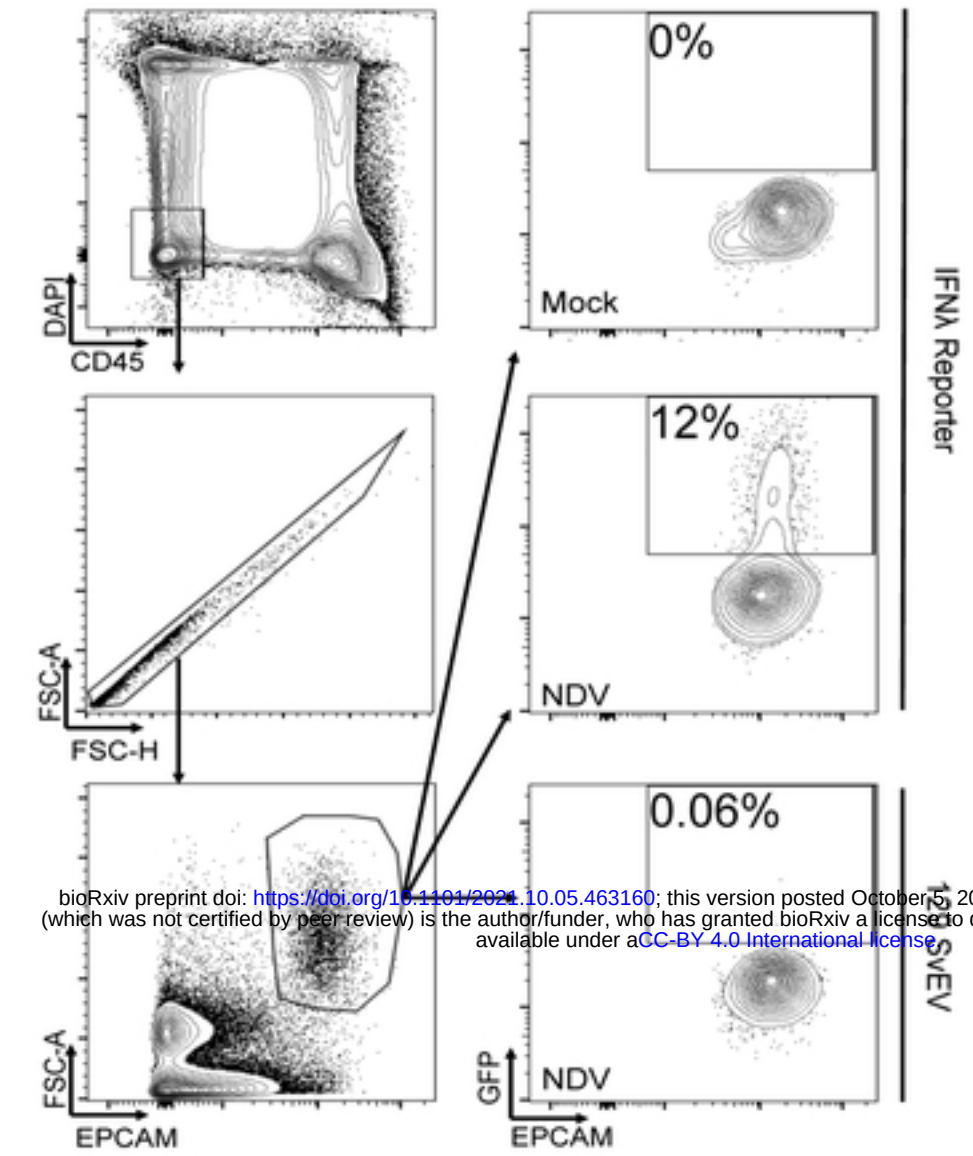

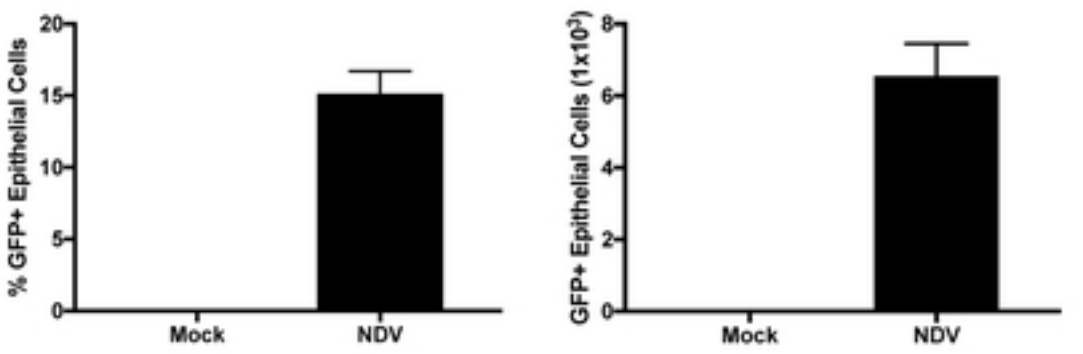

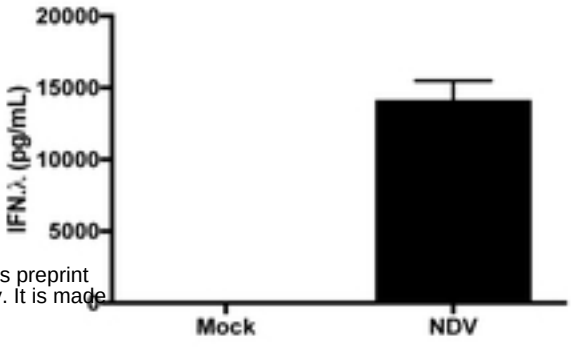

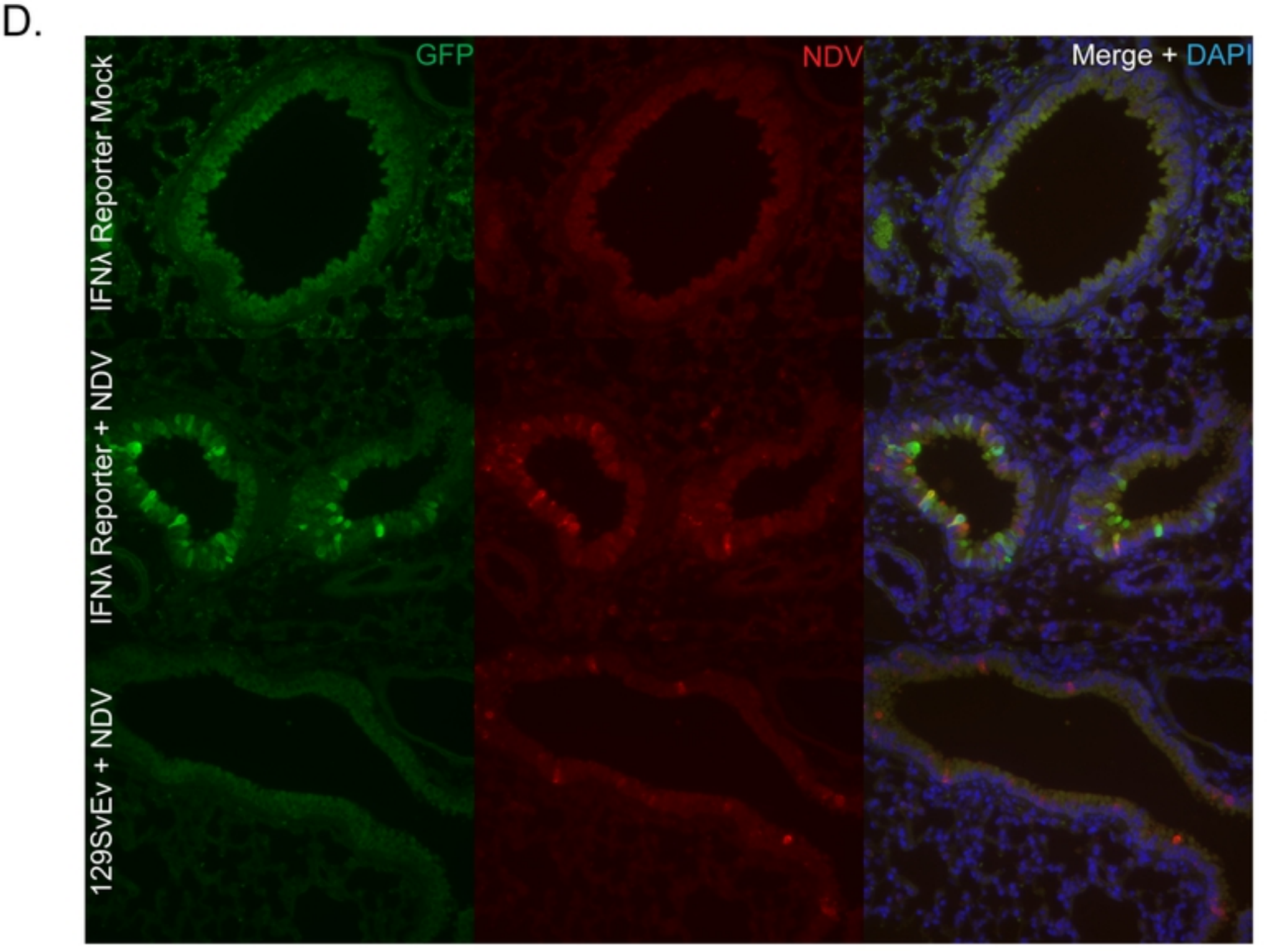

Figure

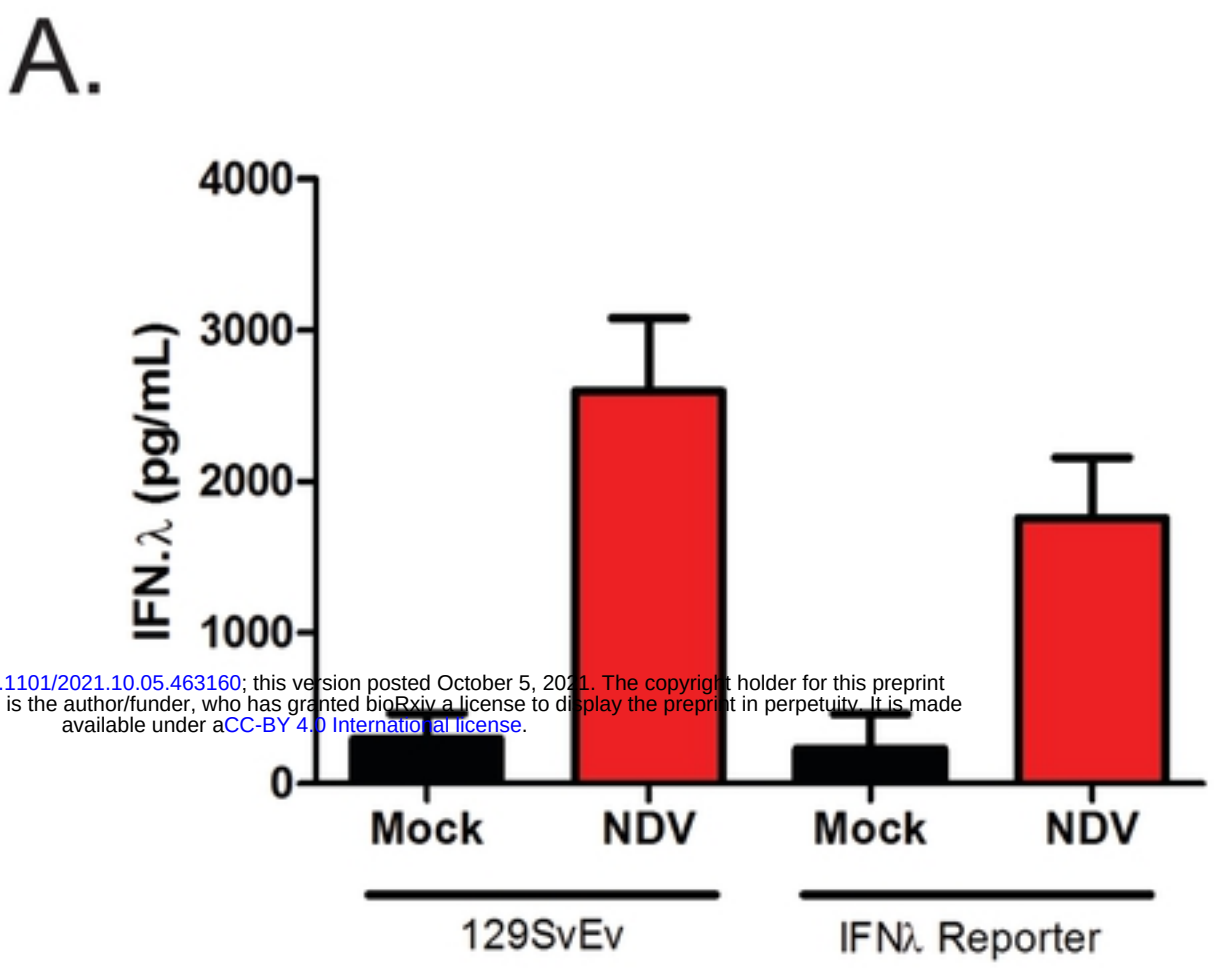

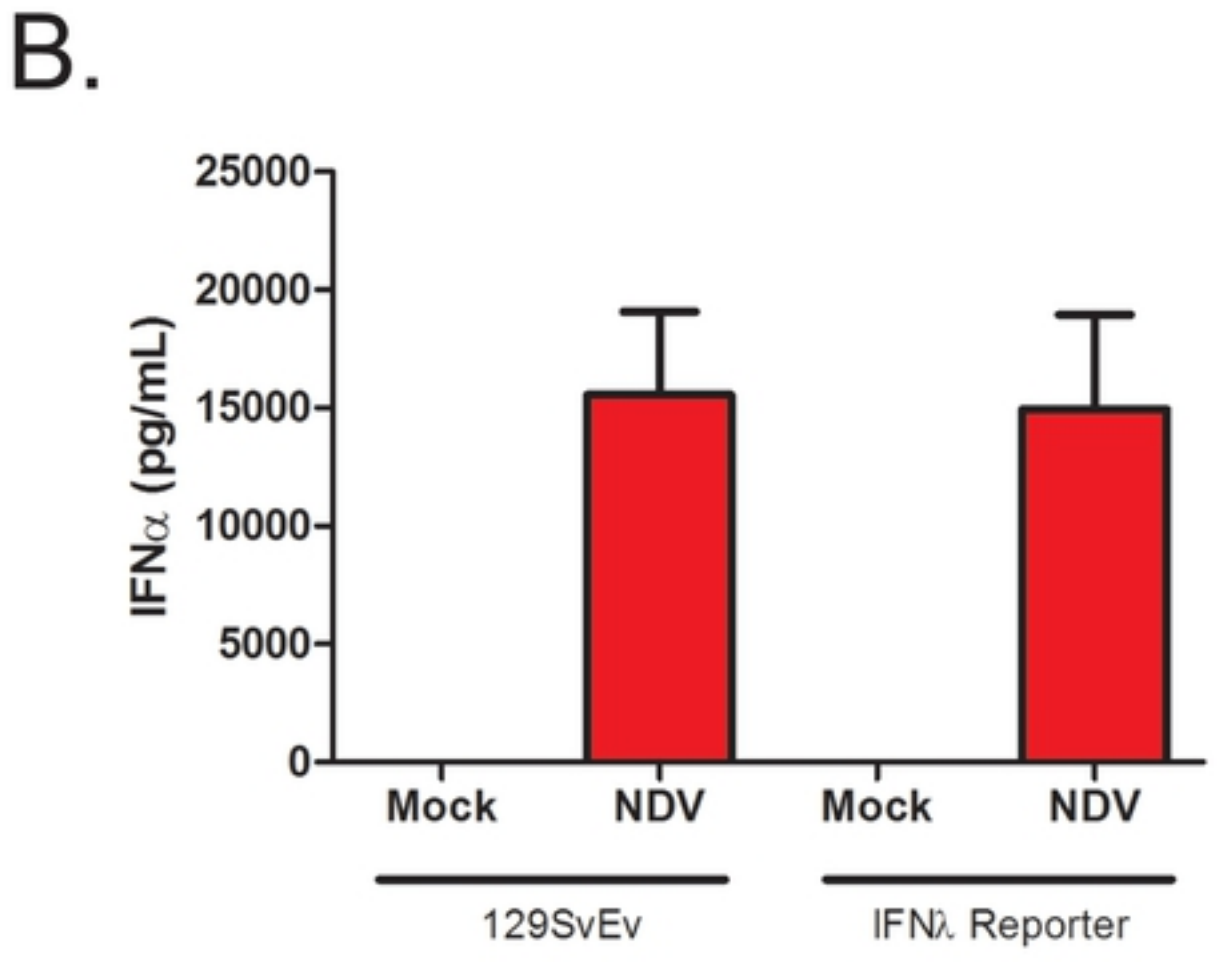

Figure

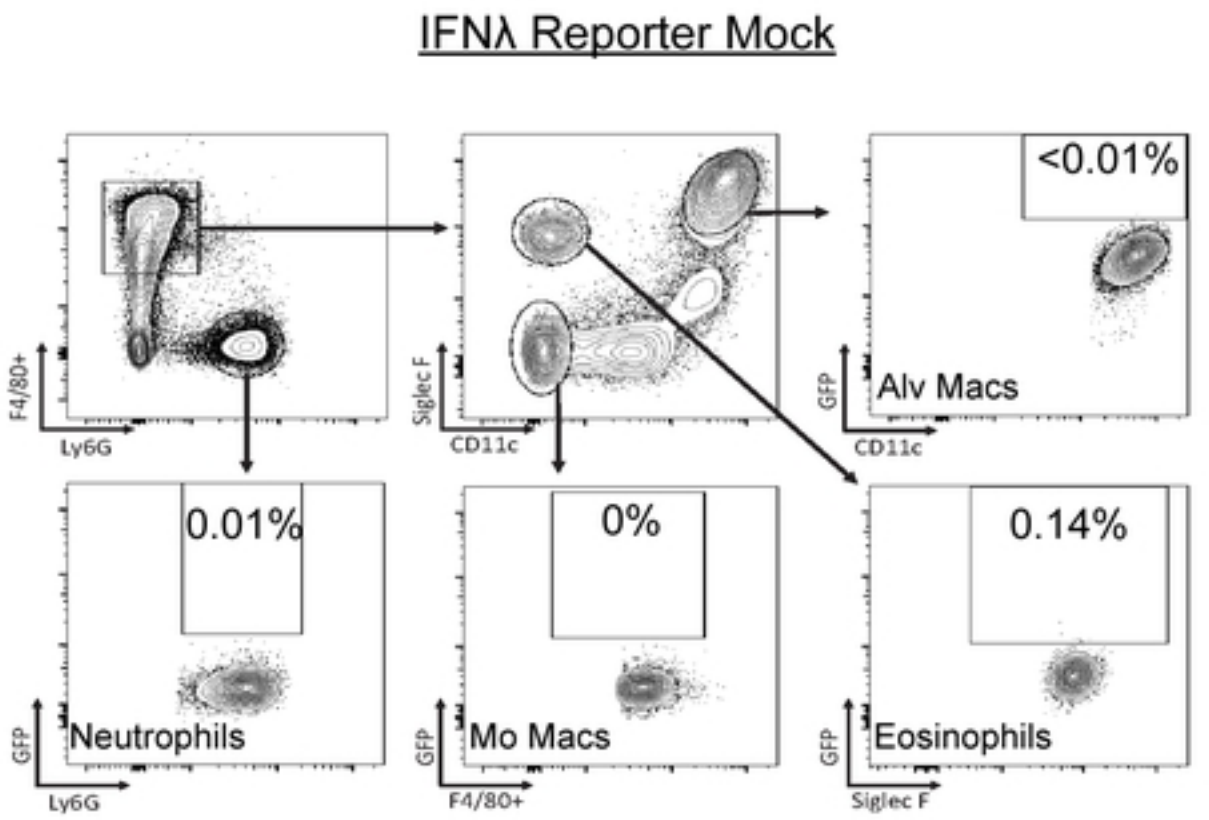

Figure

A.

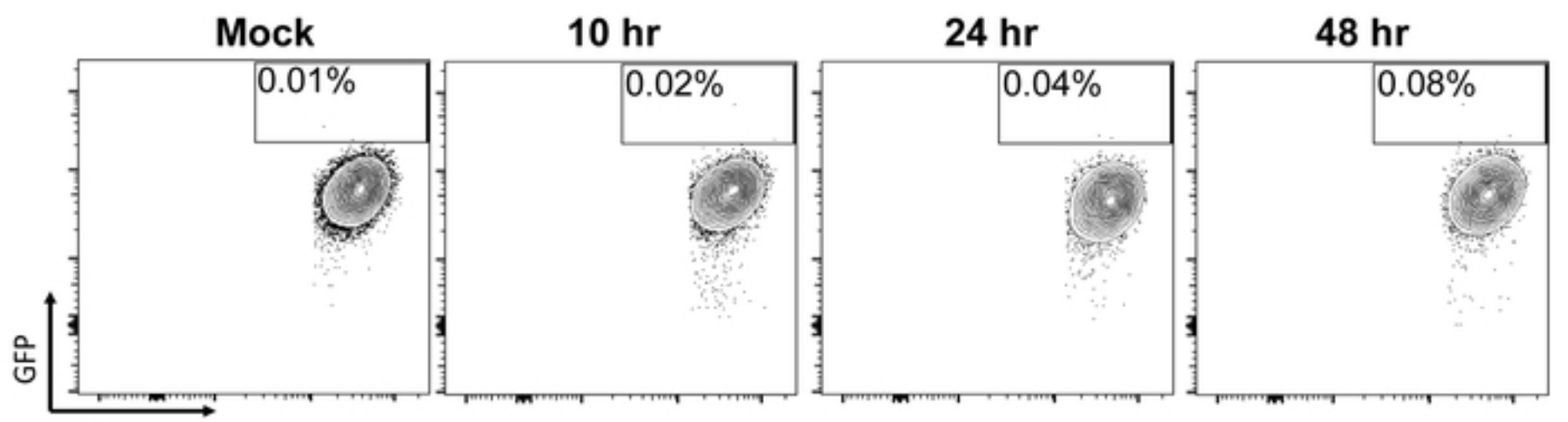

B.

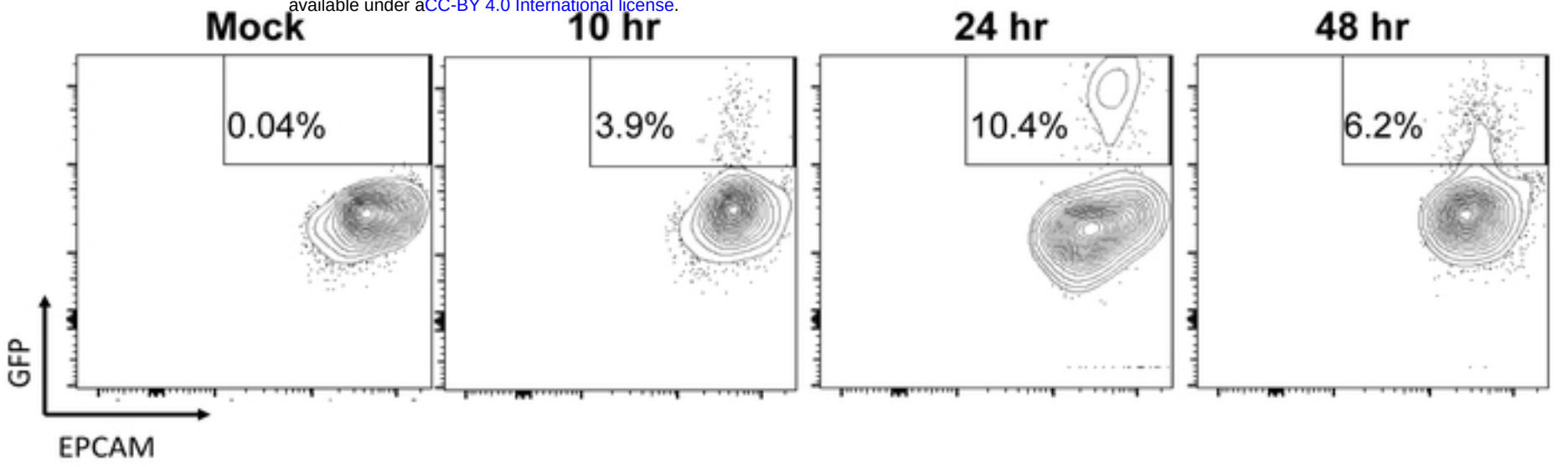

C.

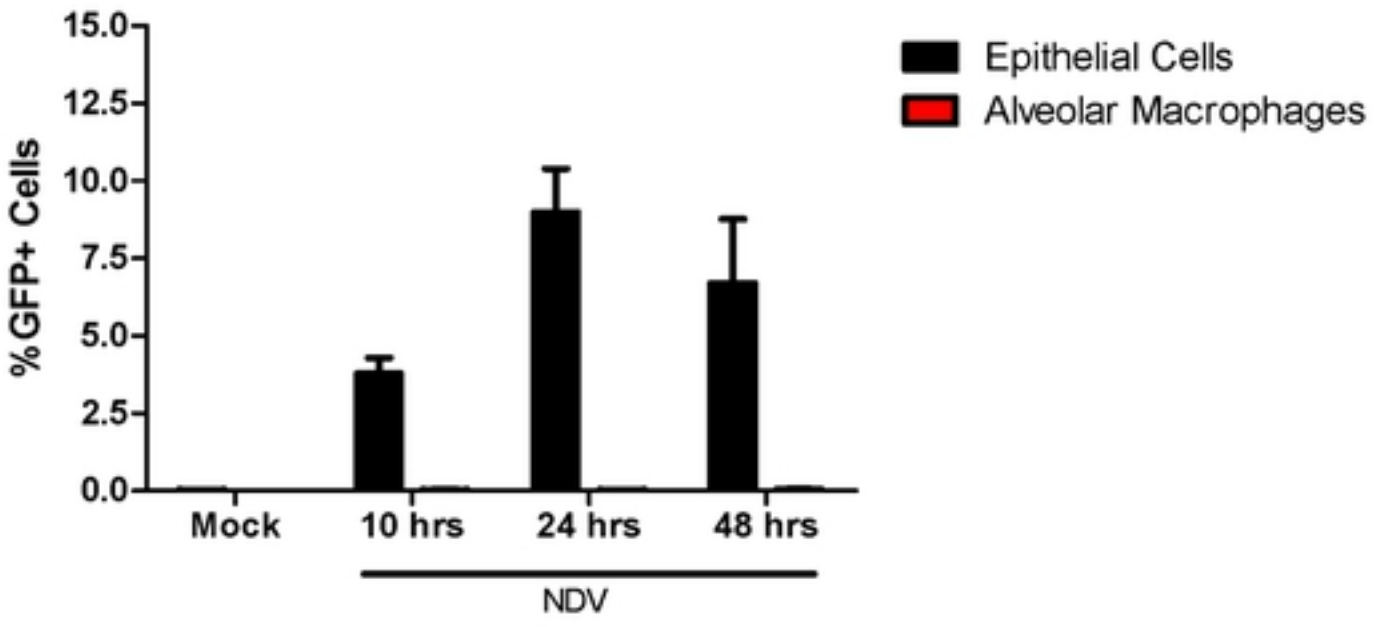

Figure

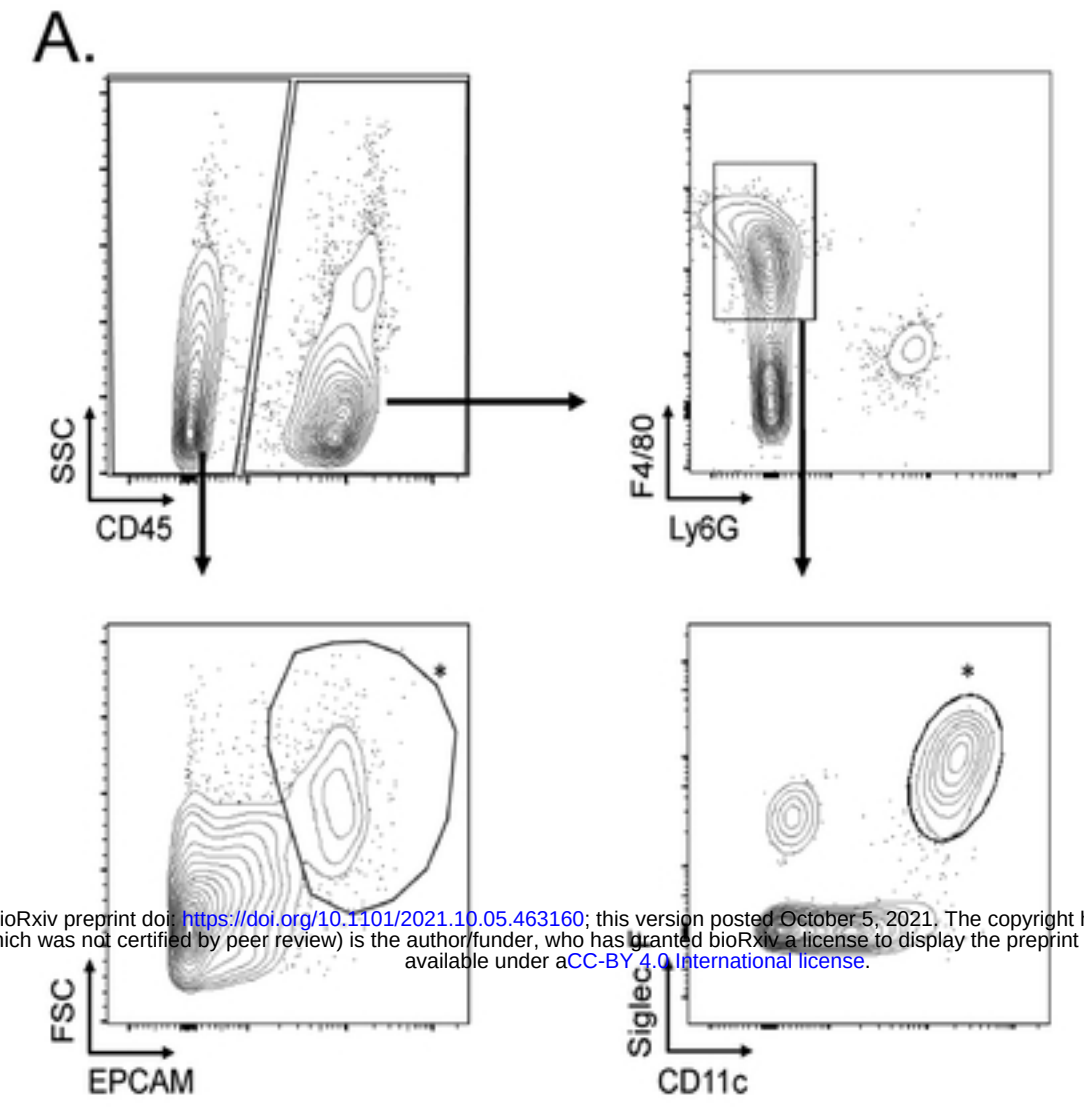

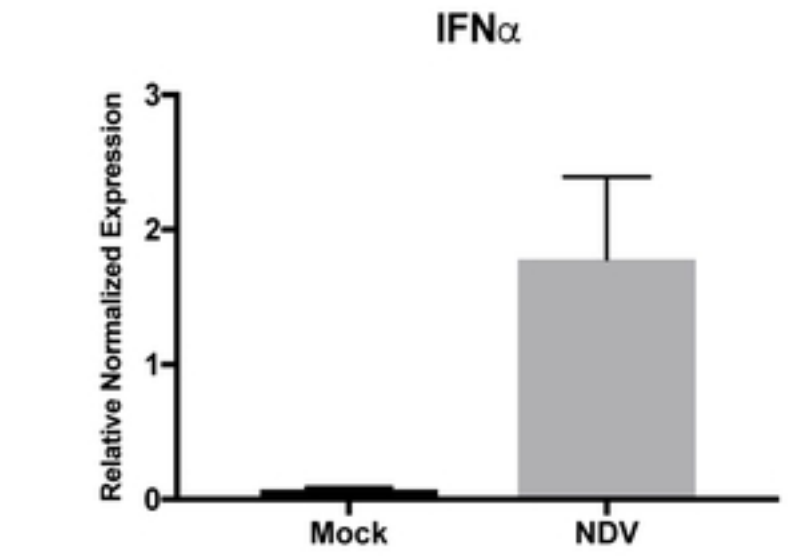

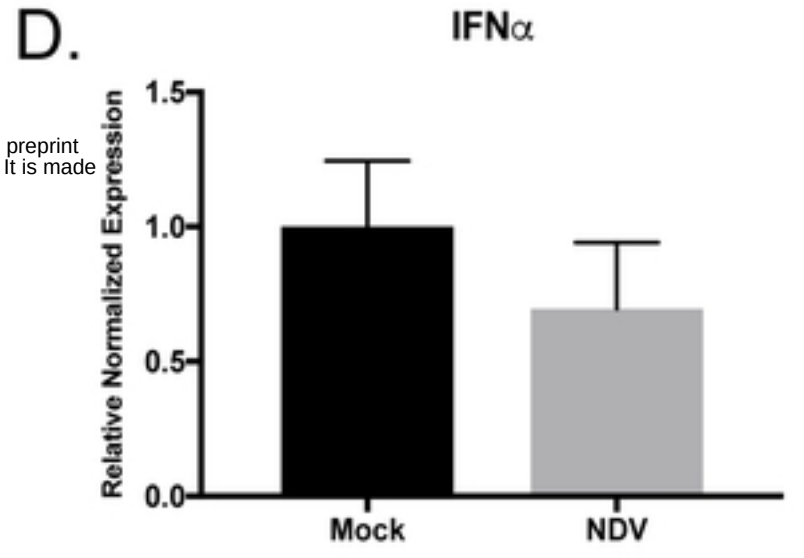

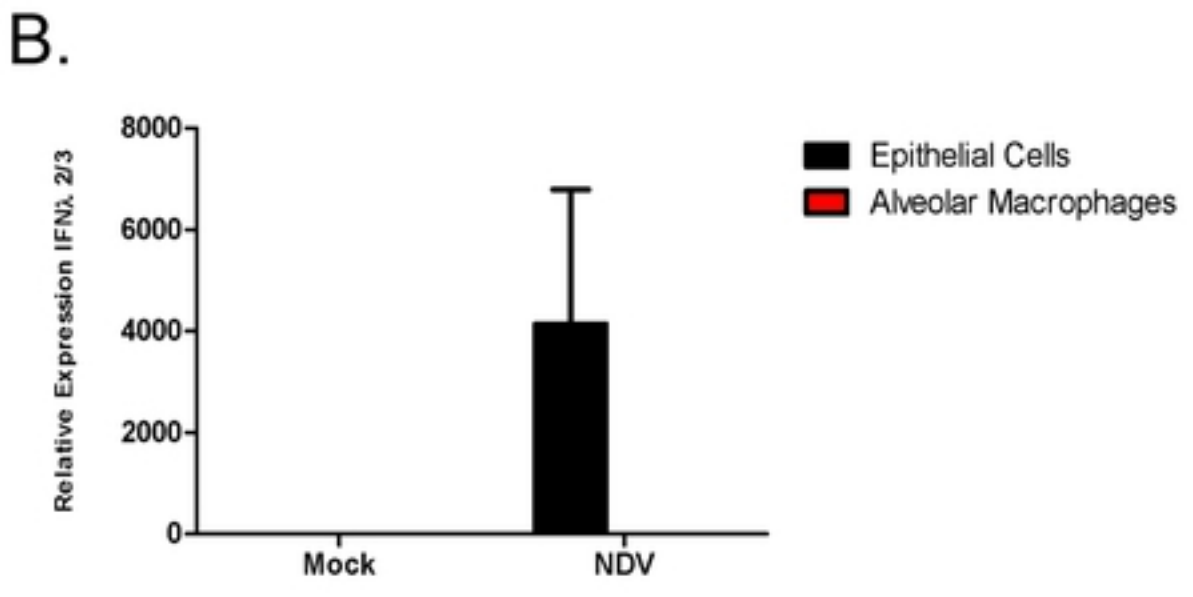

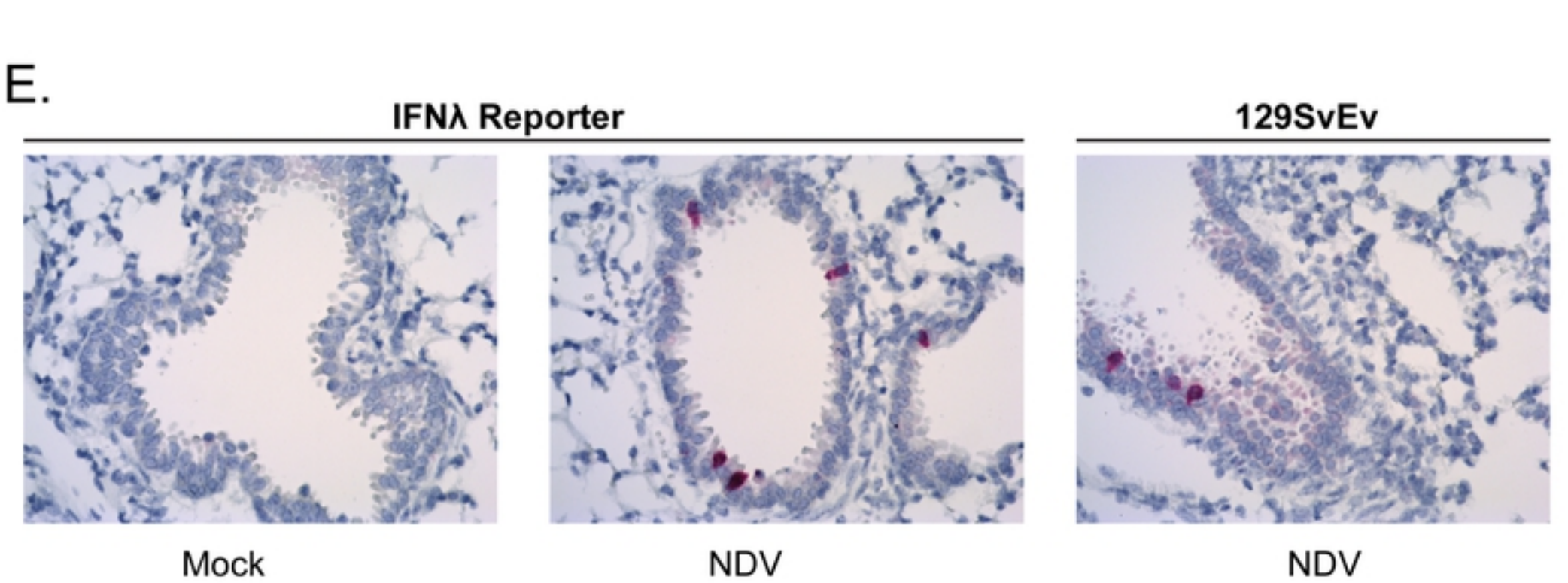

Figure

A.

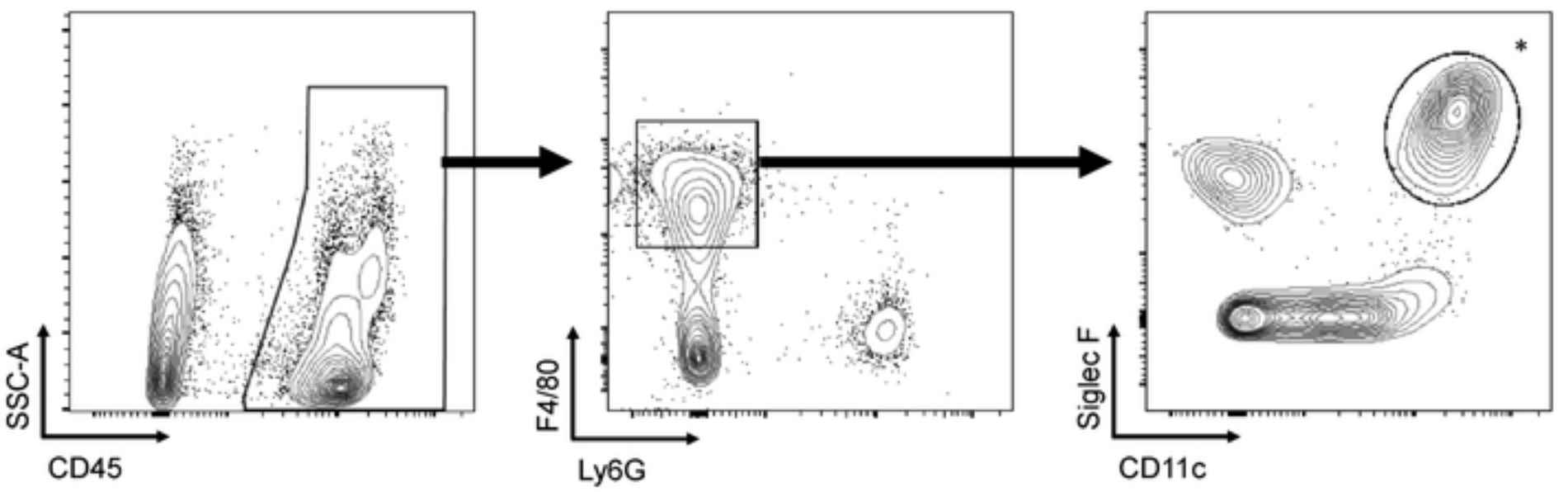

B.

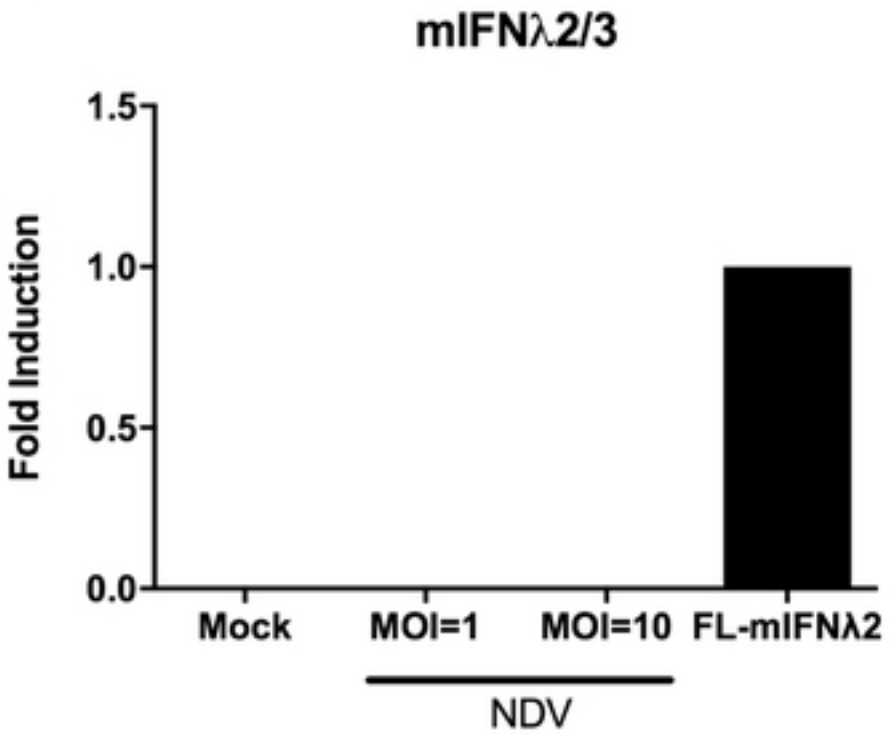

C.

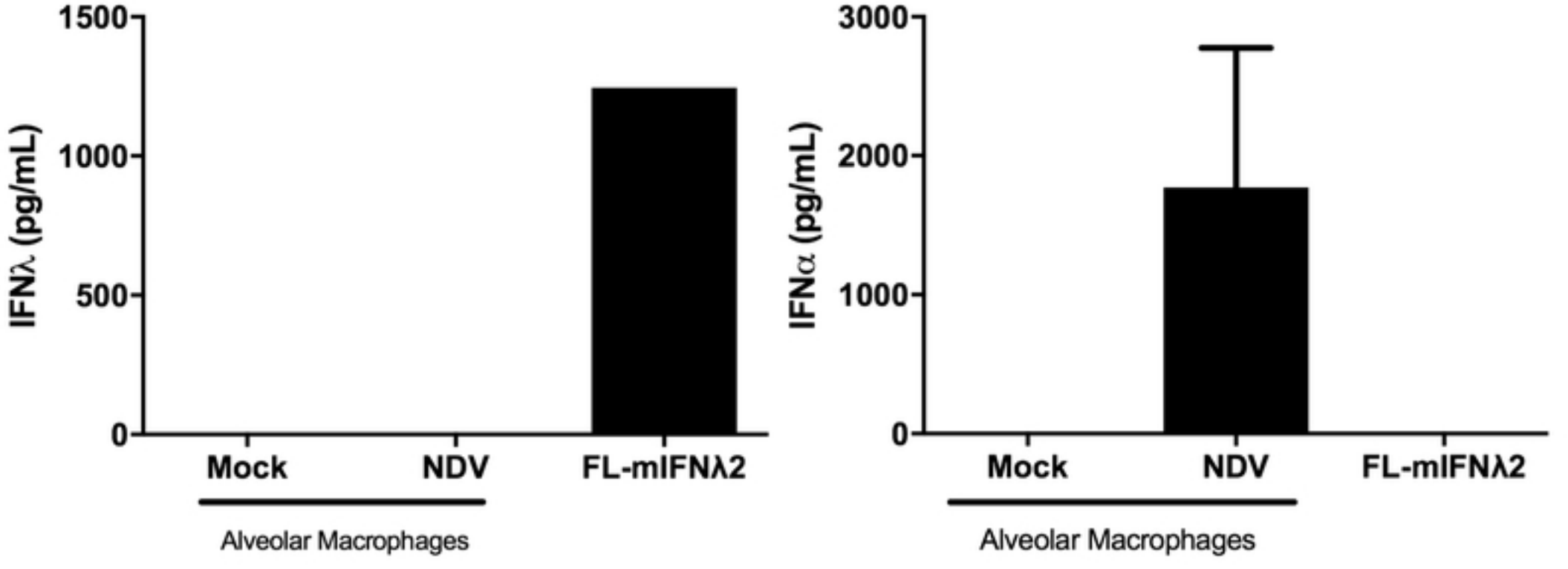

Figure

A

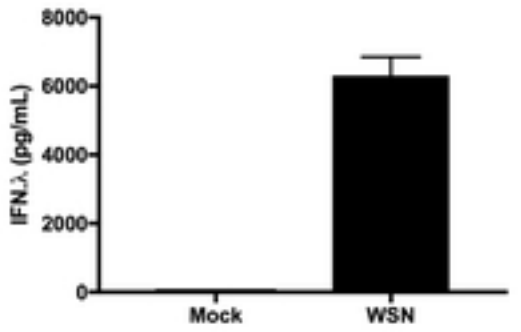

B.

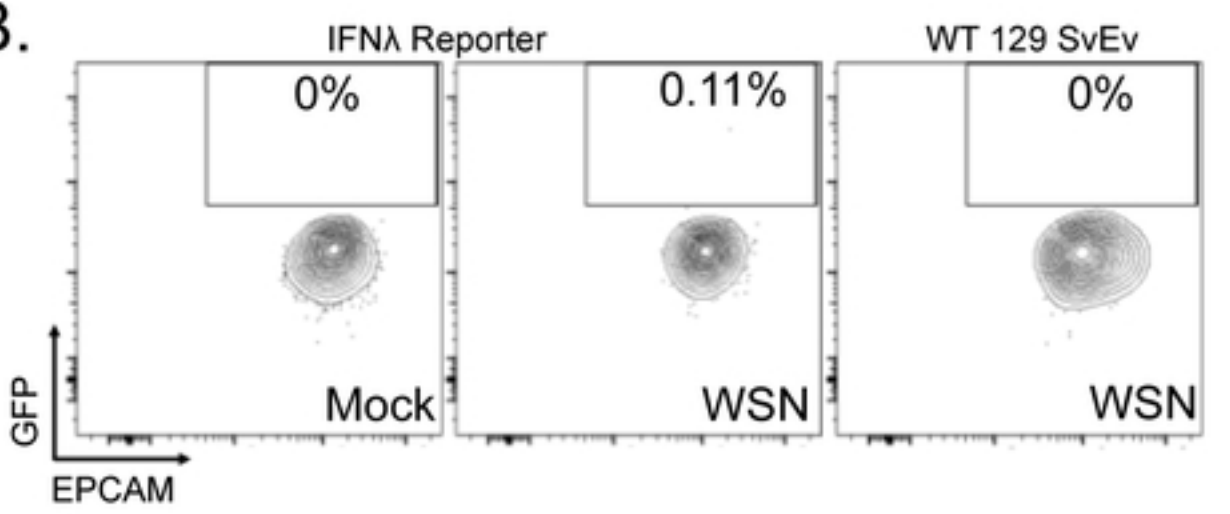

C.

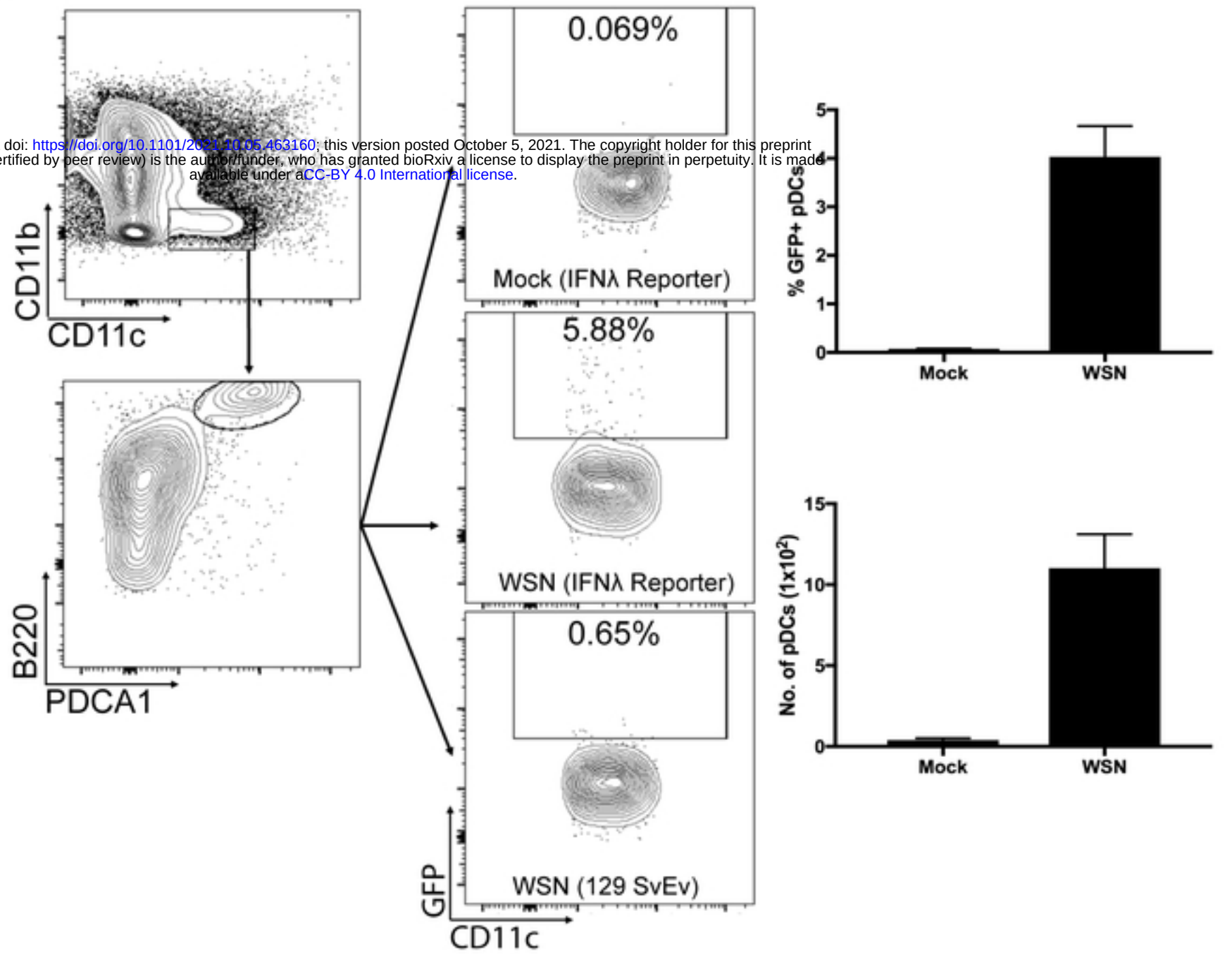

D.

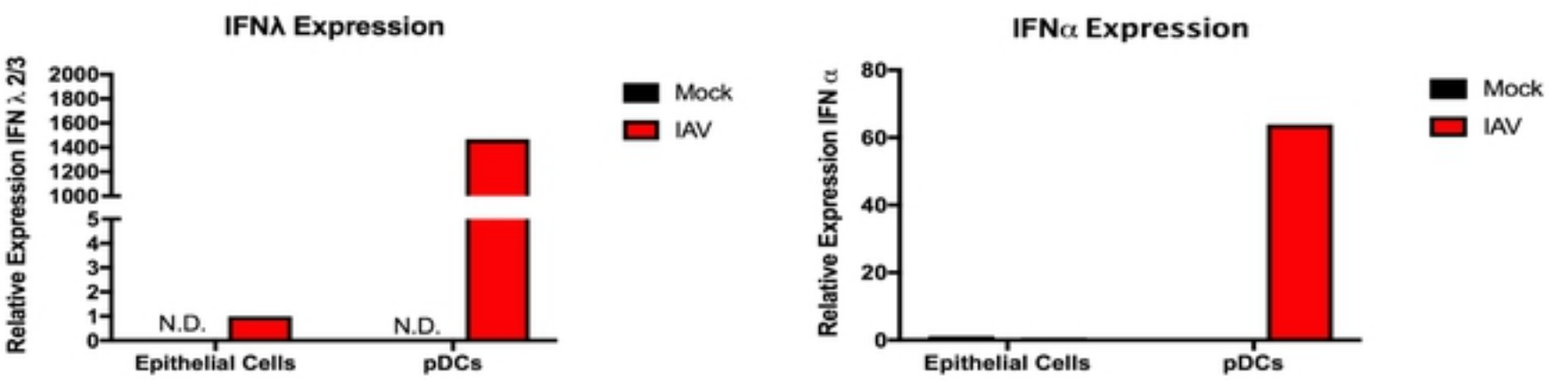

Figure

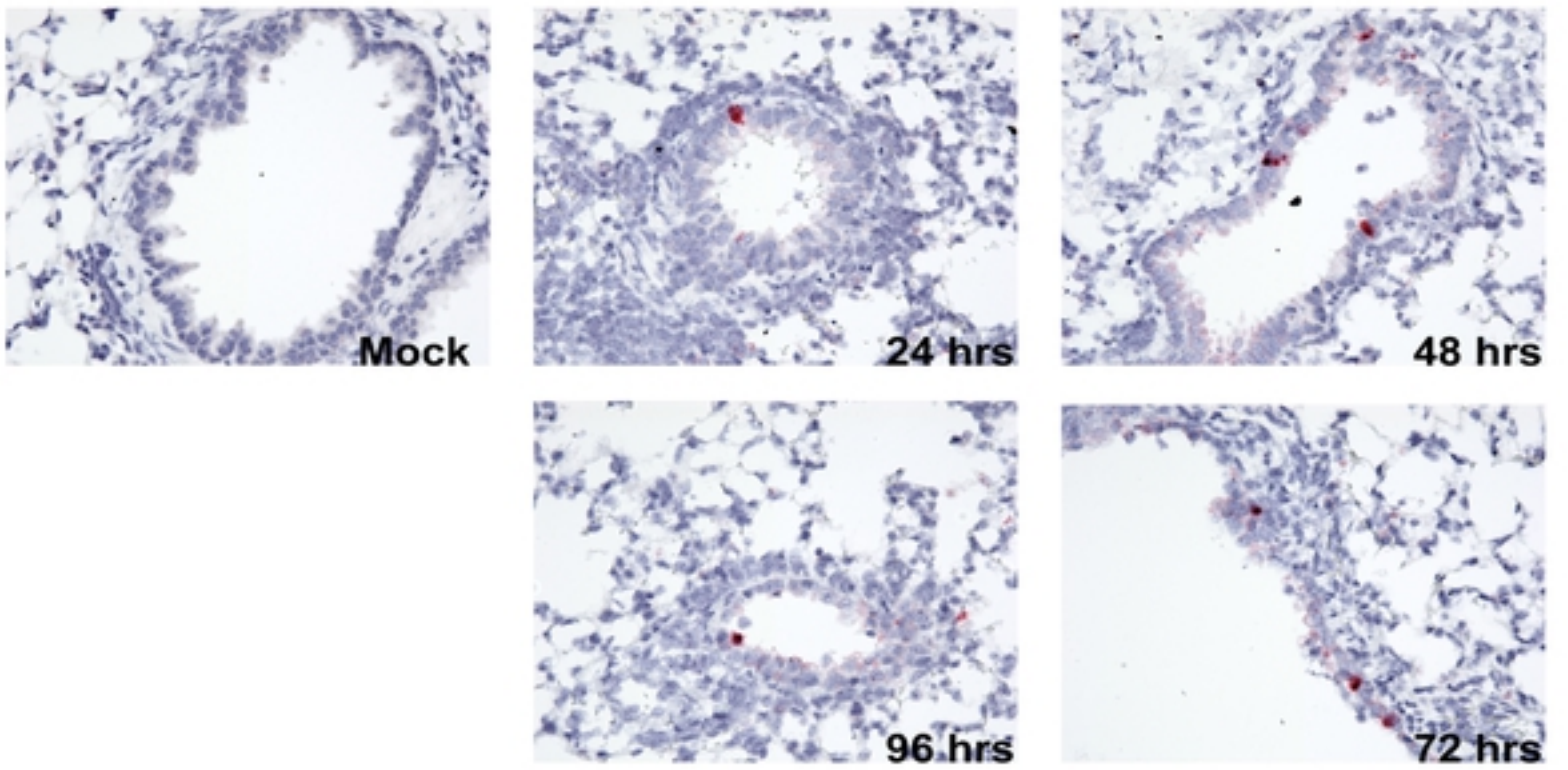

Figure

A.

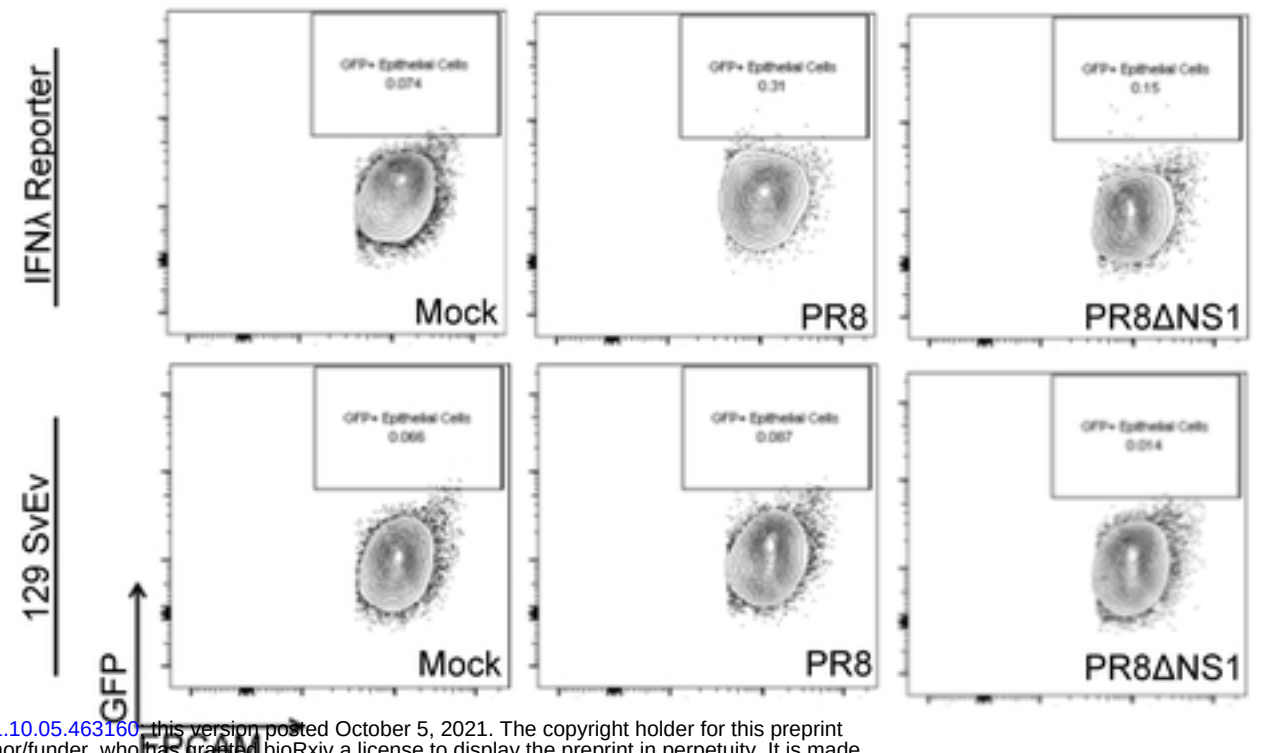

B.

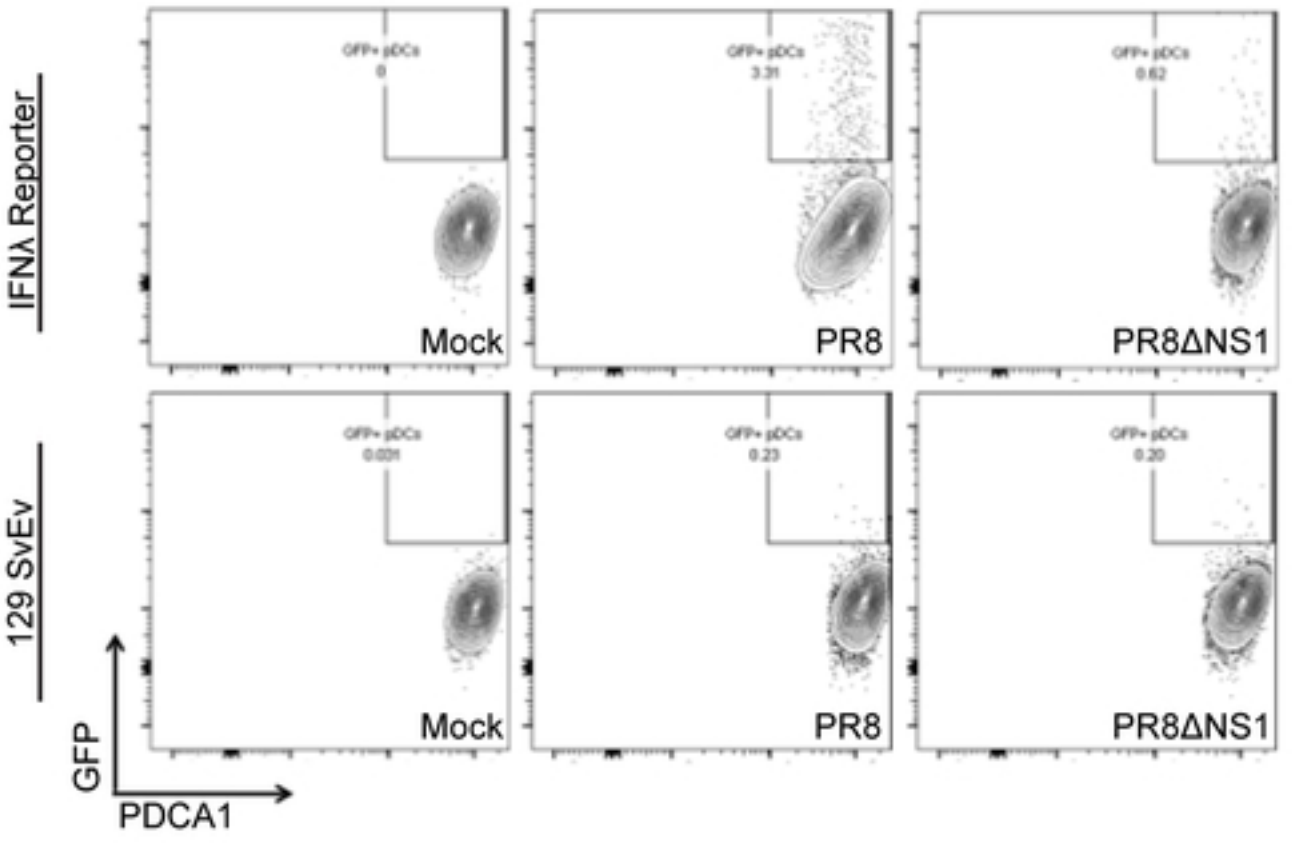

C.

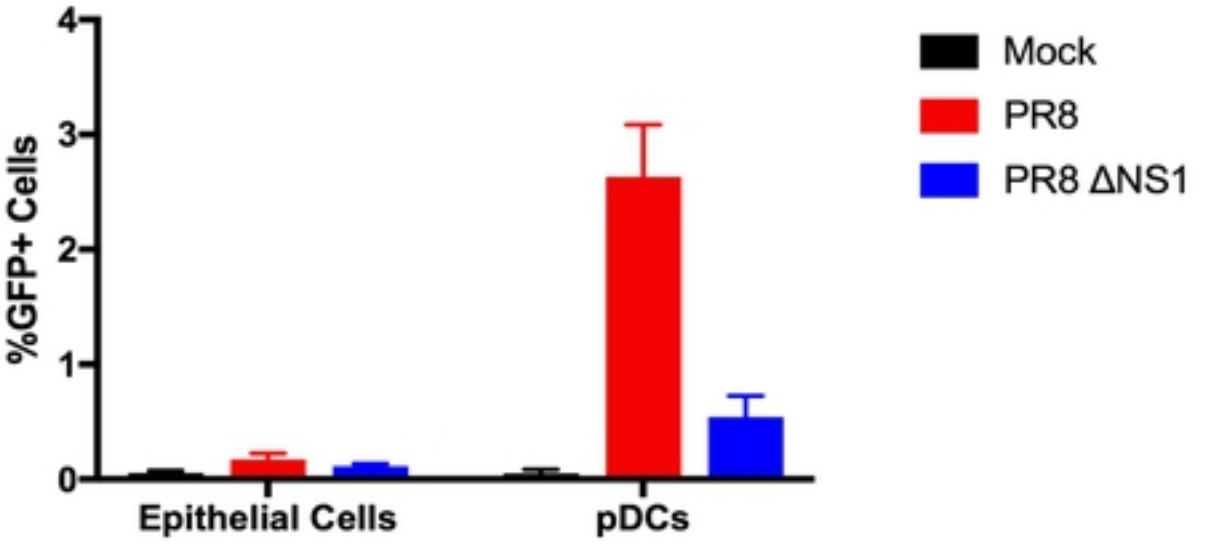

Figure

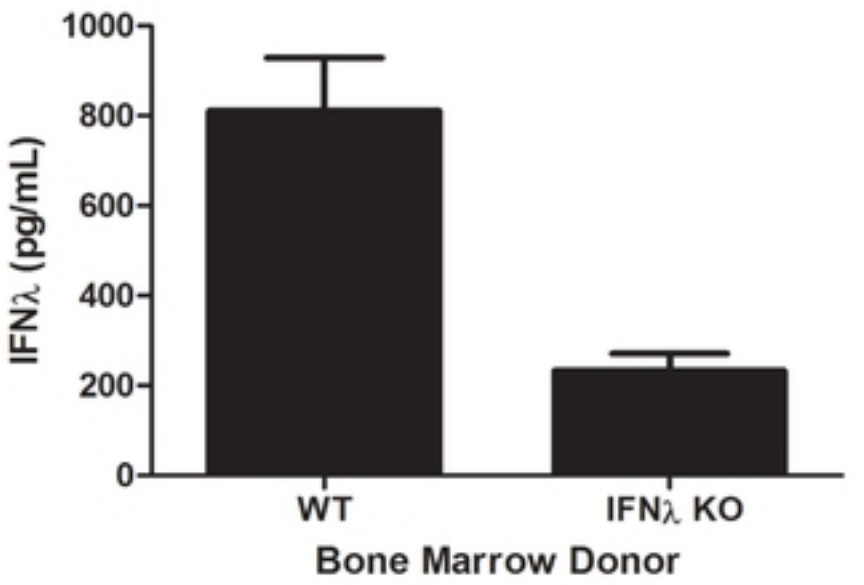

Figure

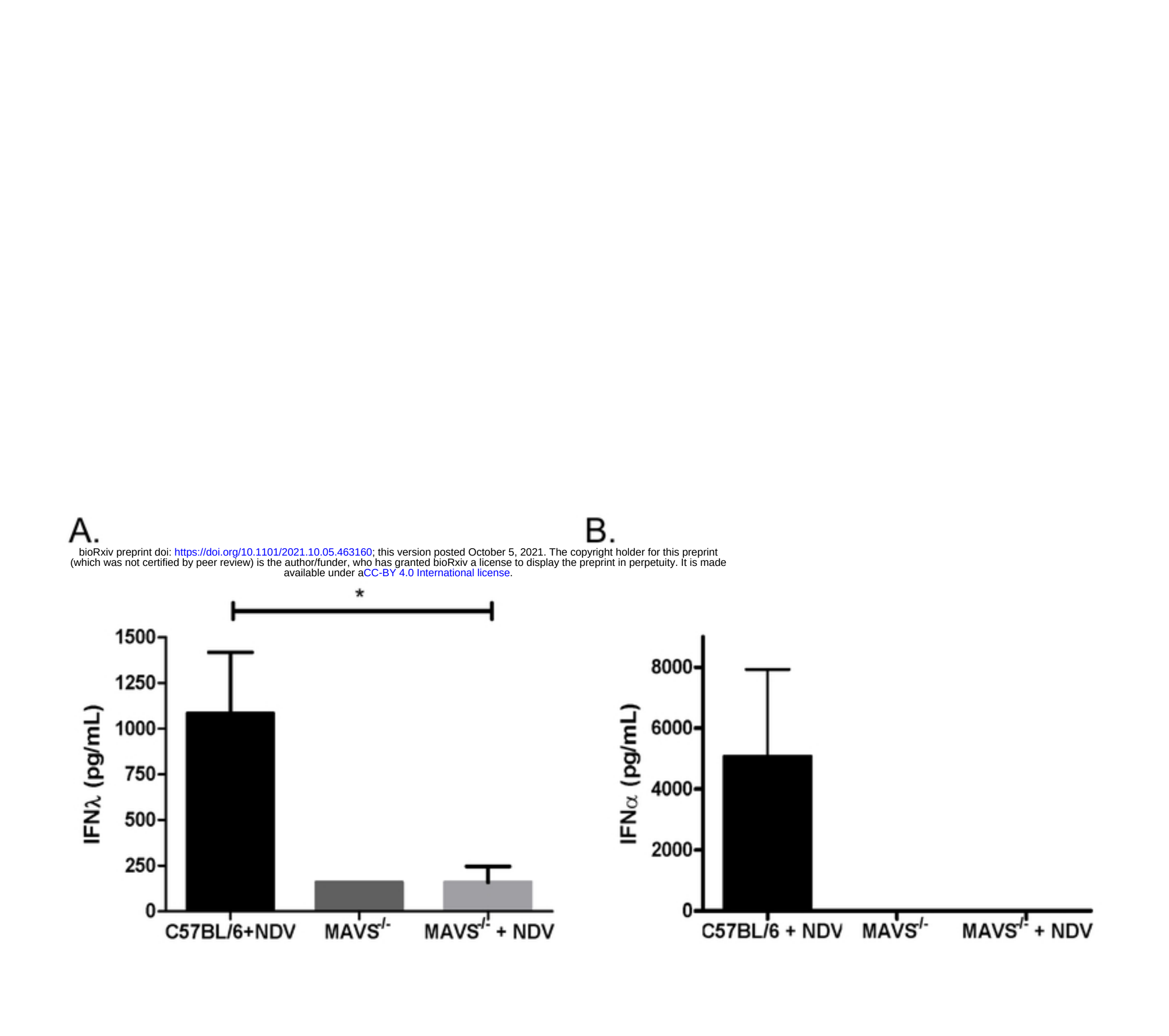

Figure

A.

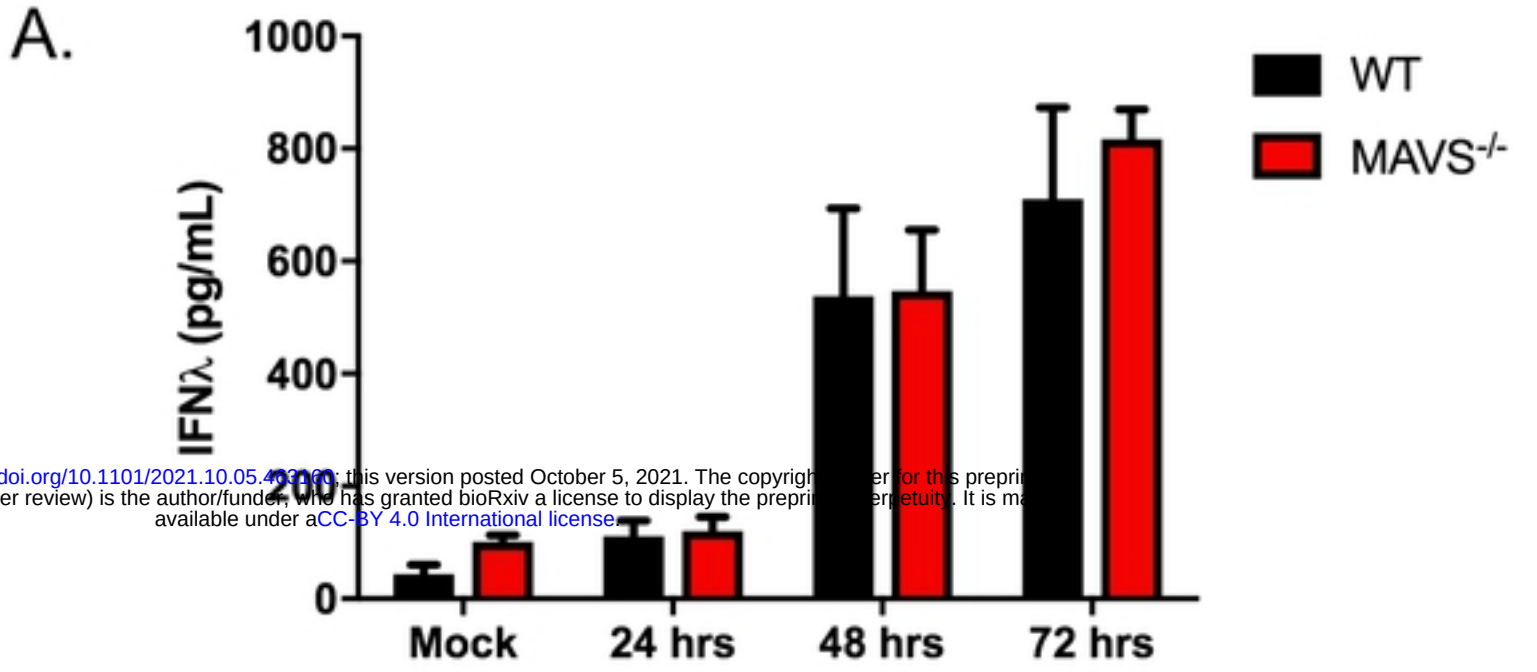

B.

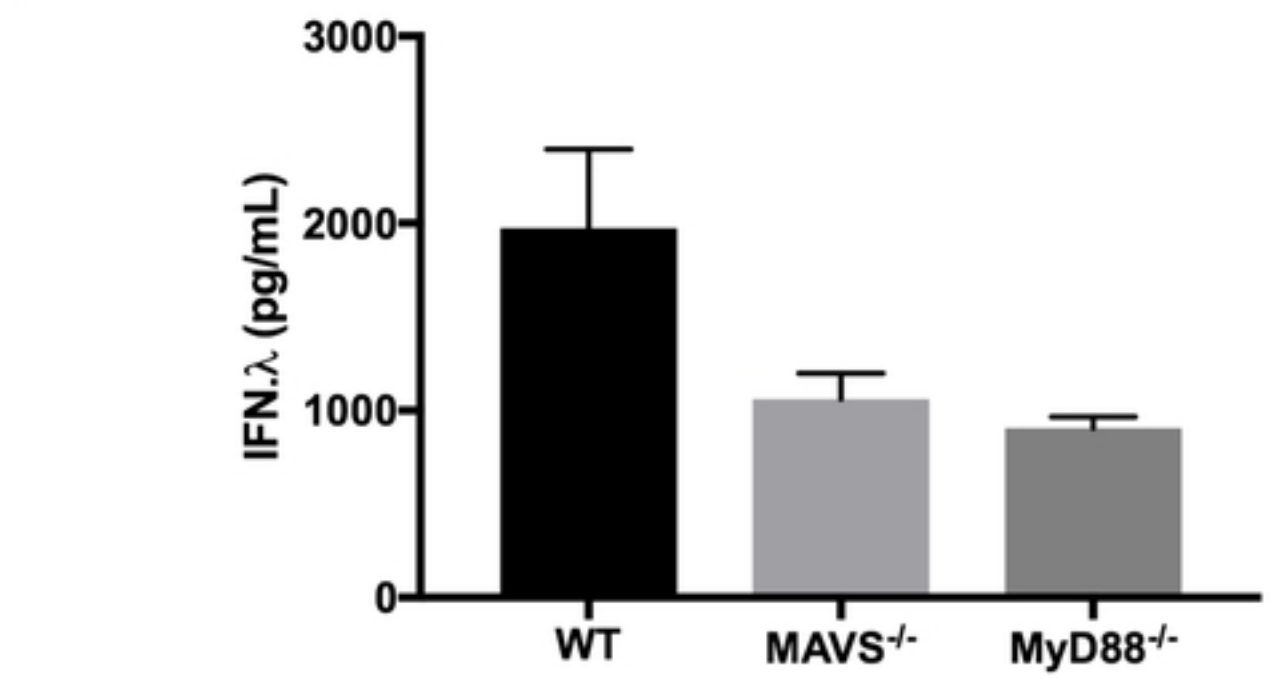

Figure

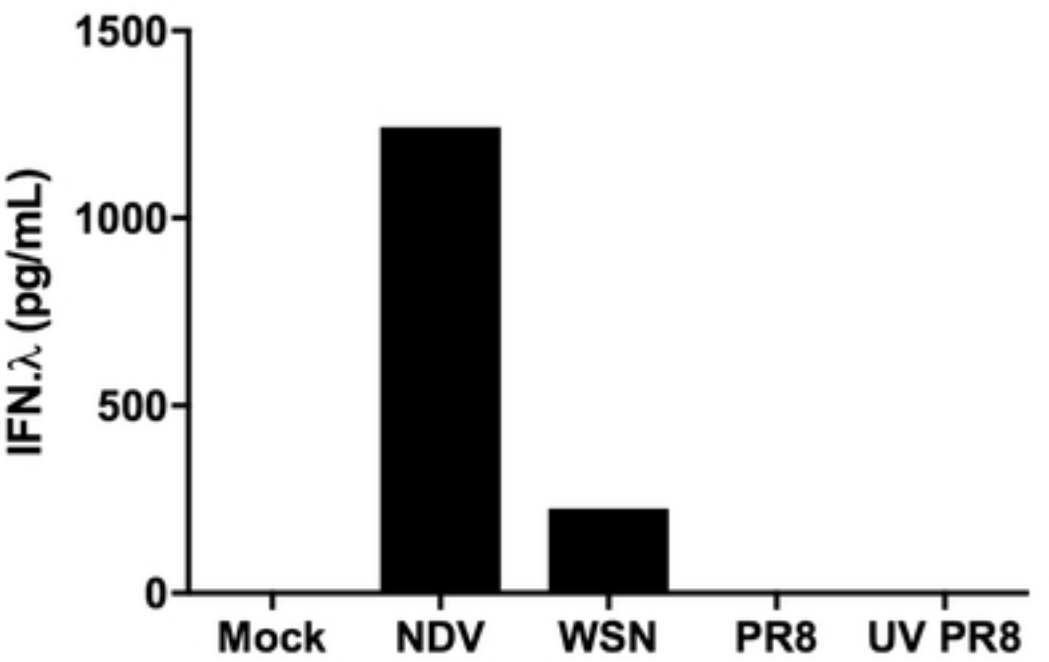

Figure

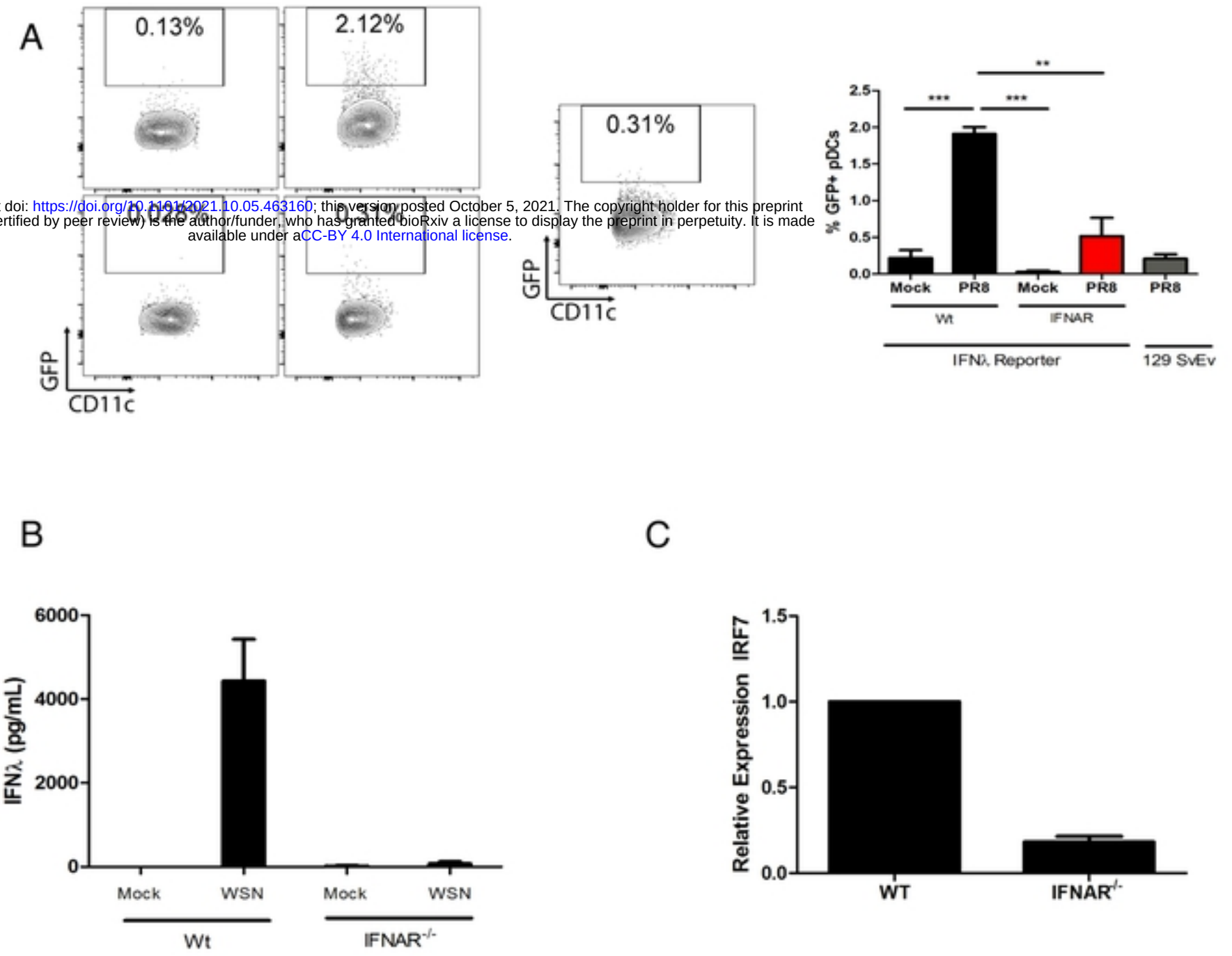

Figure

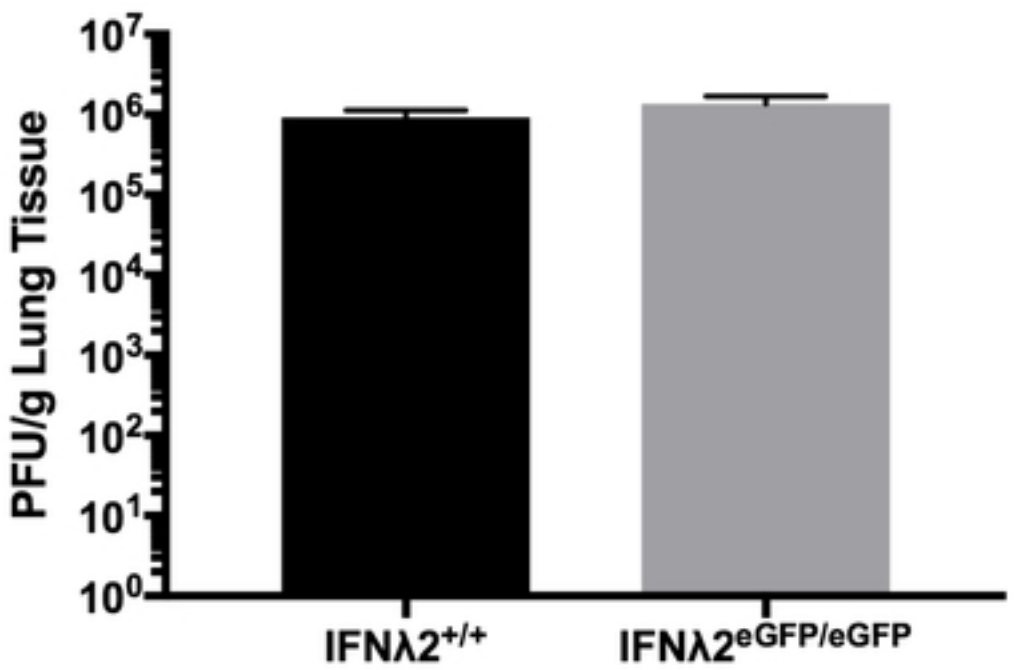

Figure

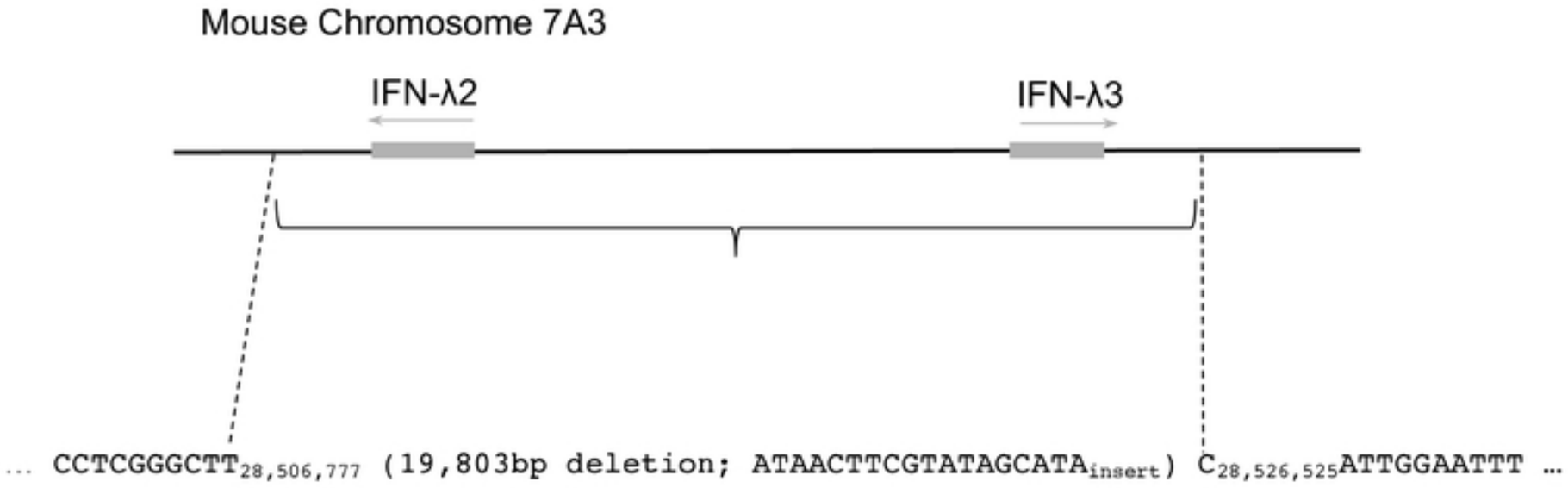

The region encompassing the IFN-λ2 and IFN-λ3 genes on murine chromosome 7, that was deleted by the Crispr/Cas9 Technology, is schematically shown.

Figure

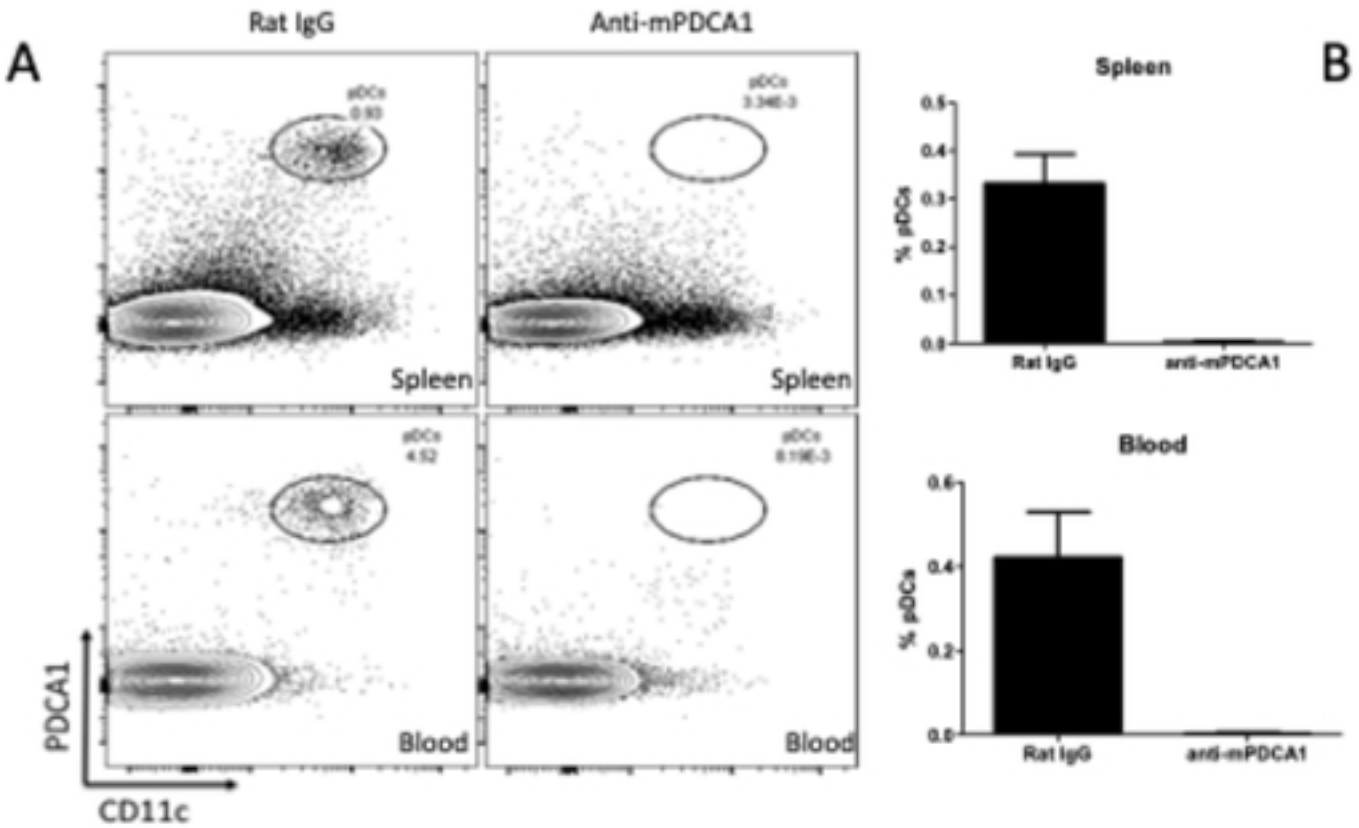
A
Rat IgG
Anti-mPDCA1
pDCs
0.93
pDCs
3.34E-3
Spleen
Spleen
pDCs
4.52
pDCs
8.19E-3
Blood
Blood
PDCA1
CD11c
Spleen
% pDCs
0.5
0.4
0.3
0.2
0.1
0.0
Rat IgG
anti-mPDCA1
Blood
% pDCs
0.6
0.4
0.2
0.0
Rat IgG
anti-mPDCA1
B
***
IFNλ (pg/mL)
1500
1000
500
0
Rat IgG
anti-mPDCA1

Figure

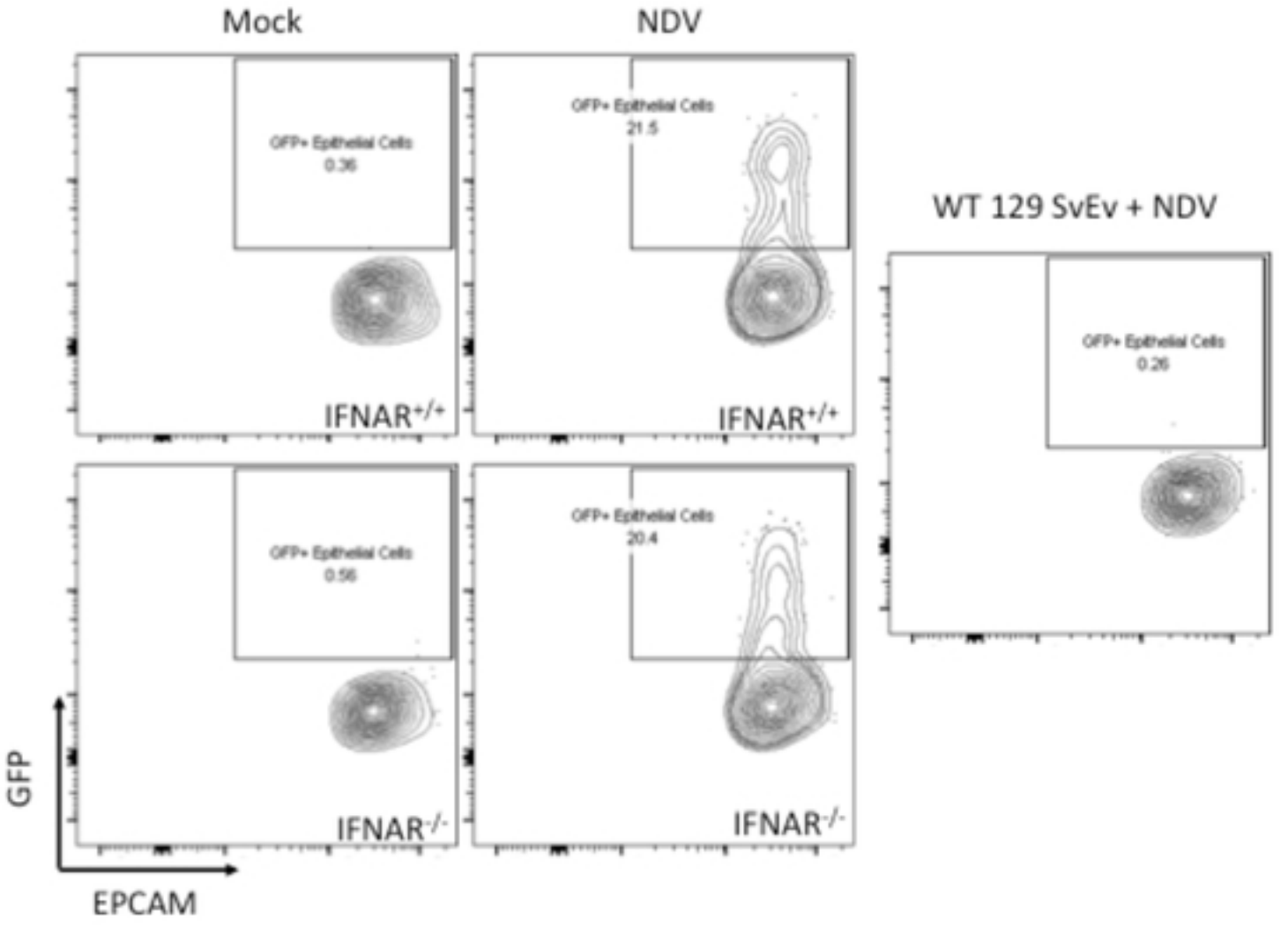
Mock
NDV
WT 129 SvEv + NDV
GFP+ Epithelial Cells
0.36
GFP+ Epithelial Cells
21.5
GFP+ Epithelial Cells
0.26
IFNAR+/+
IFNAR+/+
GFP+ Epithelial Cells
0.56
GFP+ Epithelial Cells
20.4
IFNAR-/-
IFNAR-/-
GFP
EPCAM

Figure